MSEL

Materials Science and Engineering Laboratory

MATERIALS RELIABILITY

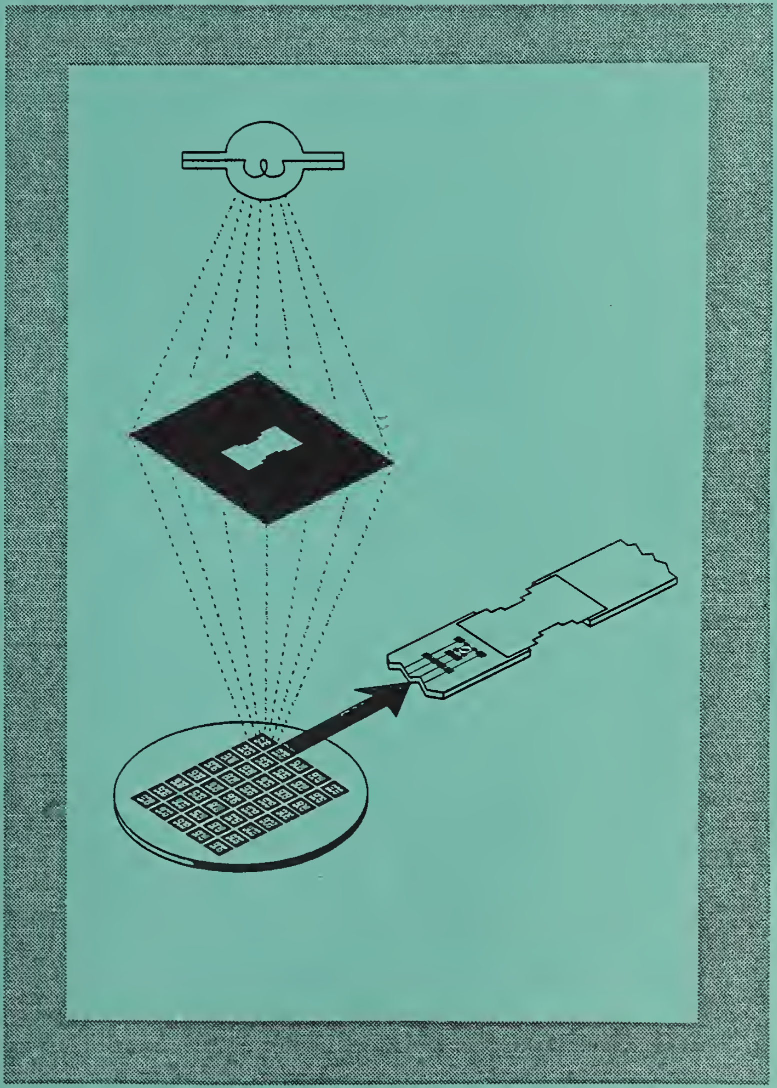

NAS-NRC
Assessment Panel
January 31-February 1, 1991

NISTIR 90-4395
U.S. Department of Commerce
National Institute of Standards
and Technology

Technical Activities 1990

Thin-film tensile specimen and silicon grips with integrated piezoresistive bridge for force measurement, under development for characterization of mechanical properties of materials in advanced electronic devices.

MSEL

Materials Science and Engineering Laboratory

MATERIALS RELIABILITY

H.I. McHenry, Chief
C.M. Fortunko, Deputy

NAS-NRC
Assessment Panel
January 31-February 1, 1991

NISTIR 4395
U.S. Department of Commerce
National Institute of Standards
and Technology

Technical Activities 1990

U.S. DEPARTMENT OF COMMERCE, Robert A. Mosbacher,Secretary
National Institute of Standards and Technology, John W. Lyons, Director

CONTENTS

DIVISION ORGANIZATION

Harry I. McHenry, Chief
(303) 497-3268

Christopher M. Fortunko
Deputy Division Chief
(303) 497-3062

PERFORMANCE	
Fracture	David T. Read (303) 497-3853
Nondestructive Evaluation	Alfred V. Clark, Jr. (303) 497-3159
Composites	Christopher M. Fortunko (Acting) (303) 497-3062
PROPERTIES	
Cryogenic Materials	Richard P. Reed (303) 497-3870
Physical Properties	Hassel M. Ledbetter (303) 497-3443
PROCESSING	
Welding	Thomas A. Siewert (303) 497-3523
Thermomechanical Processing	Yi-Wen Cheng (303) 497-5545
ADMINISTRATIVE SUPPORT	
Administrative Officer	Kathy S. Sherlock (303) 497-3288
Division Secretary	Heidi M. Quartemont (303) 497-3251
Group Secretaries	Vonna E. Ciaranello (303) 497-5338 Dawn T. Lewis (303) 497-3290

INTRODUCTION

MATERIALS RELIABILITY DIVISION

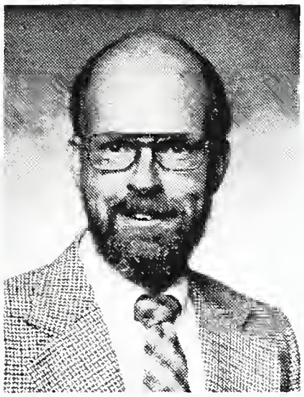

Harry I. McHenry
Chief

Christopher M. Fortunko
Deputy Chief

The Materials Reliability Division conducts materials research to improve the quality, reliability, and safety of industrial products and the nation's infrastructure. Our research fosters the use of advanced materials in commercial products by improving confidence in their service performance. We do this by developing measurement technology for:

1. process control which improves the quality, consistency and producibility of materials,

2. nondestructive evaluation (NDE) which assures the quality of finished materials and products,

3. fitness-for-purpose standards which relate material quality to reliability and safety, and

4. materials evaluation for severe applications, particularly for service at cryogenic temperatures.

Our interdisciplinary staff is organized into specific research groups in the general areas of materials performance, properties, and processing. Each group is headed by a recognized expert in that technology who provides a focal point for industrial cooperations, scientific interactions, and technology transfer.

This year was our first as the Materials Reliability Division; formerly we were the Fracture and Deformation Division. The new name describes our research goals and better reflects the NIST mission: "to assist industry in the development of technology and procedures needed to improve quality, to modernize manufacturing processes, to ensure product reliability ... based on new scientific discoveries." In support of the long-range plan of the Materials Science and Engineering Laboratory, our new programs focus on advanced materials with high commercial potential and on automated processing, which is the key to improved productivity in the materials industry. We also conduct materials research for other government agencies and provide technical services to industries, universities, and other scientific laboratories.

American industry leads the world in the development of advanced materials, but frequently we trail in using these materials for commercial products. The commercial lag is due to lack of confidence in the service performance of advanced materials, particularly safety and reliability. The Materials Reliability Division's programs are developing measurement methods, sensors, standards, and reference data that will be used to measure the quality of advanced materials and to assess their service performance. Once measurement methods and standards are developed, industry can confidently use advanced materials to design and manufacture new products.

SELECTED HIGHLIGHTS
MATERIALS RELIABILITY DIVISION

Composites NDE: A high resolution ultrasonic system has been developed for inspecting thick polymer-matrix composites. The high dynamic range (60 dB) and large band width (60 kHz to 60 MHz) of the new system permits characterization of material property variations and detection of flaws.

NDE Instruments: Field trials were conducted on two prototype ultrasonic NDE instruments. A formability sensor system was delivered to the Ford Motor Company for evaluation at their Dearborn stamping plant. An ultrasonic system for roll-by inspection of railroad wheels is being evaluated at the American Association of Railroads test track in Pueblo, Colorado.

Elastic Waves in Composites: A powerful technique using a time-dependent Green's function method has been developed for studying propagation of elastic waves and their scattering from discontinuities in anisotropic solids. This three-dimensional theory will provide a useful framework for design of NDE experiments as well as interpretation of NDE data on composite materials.

Electronic Packaging: Computer programs have been developed to convert coordinate points on solder joint surfaces obtained by x-ray laminography and optical inspection into finite element meshes for stress analysis. Automated stress analysis will permit rapid assessment of the significance of geometric irregularities on the reliability of solder joints in electronic packages.

Thermomechanical Processing: The continuous cooling transformation (CCT) characteristics and the high-temperature, high strain-rate flow properties were measured for microalloyed SAE 1141 forging steel. We measured the effects of deformation on the CCT curve for conditions simulating direct forging.

Charpy Standards: In cooperation with the Office of Standard Reference Materials, we provided over 1000 industrial customers with Charpy V-notch reference specimens and calibration services for certification of Charpy impact test machines to ASTM Standard E23.

Cryogenic Testing: A 5 MN (1 million pound-force) servohydraulic testing machine was refurbished and equipped with a cryostat and dewar capable of testing specimens 2 m long and 50 cm in diameter in liquid helium. It was used to perform full scale mechanical and thermal simulation of structural support struts for a superconducting magnetic energy storage project.

Aluminum-Lithium Alloys: A cooperative program with NASA indicated that aluminum-lithium alloys have sufficient oxygen compatibility for use in cryogenic tankage for the Advanced Launch System. The Air Force-sponsored program led to ten recommended changes in ASTM test procedures for mechanical-impact oxygen-compatibility testing.

Automated Welding: An intelligent welding program was initiated for the U.S. Navy in conjunction with Babcock and Wilcox and INEL. The through-arc sensing techniques being developed to characterize metal transfer have been shown to detect contact tip wear, one problem that reduces the reliability of automated welding.

Superconductors: Using an ionic-crystal model and ultra sound-velocity measurements, we studied some physical properties of the $Y_1Ba_2Cu_3O_x$ superconductor as a function of oxygen content ($x = 6-7$). We found generally good model-measurement agreement for the shear modulus and for the Debye temperature. Adding oxygen stiffens the lattice monotonically.

RESEARCH STAFF

Austin, Mark W.	• Radioscopy • Elastic properties • X-ray diffraction
Berger, J. R.	• Fracture mechanics • Photomechanics • Dynamic fracture
Cheng, Yi-Wen	• Fatigue of metals • Thermomechanical processing of steels • Ferrous metallurgy
Clark, Alfred V., Jr.	• Ultrasonic NDE • Engineering mechanics • Nondestructive evaluation
Fitting, Dale W.	• Sensor arrays for NDE • Ultrasonic and radiographic NDE • NDE of composites
Fortunko, Christopher M.	• Ultrasonic transducers and instrumentation • Nondestructive evaluation • Analog measurements
Kim, Sudook	• Elastic properties • Low-temperature physical properties • Ultrasonics
Ledbetter, Hassel M.	• Physical properties of solids • Theory and measurement of elastic constants • Martensite-transformation theory
Lin, Ing-Hour	• Electronic materials • Physics of fracture • Dislocation theory
McCowan, Chris N.	• Welding metallurgy • Mechanical properties at low temperatures • Metallography and fractography
McHenry, Harry I.	• Fracture mechanics • Low-temperature materials • Fracture control
Purtscher, Pat T.	• Fracture properties of metals • Metallography and fractography • Mechanical properties at low temperatures

Quinn, Timothy P.	• Control theory • Welding automation • Mechanical design
Read, David T.	• Electronic packaging • Elastic—plastic fracture mechanics • Mechanical properties of metals
Reed, Richard P. (Until 3/90; retired)	• Mechanical properties • Low-temperature materials • Martensitic transformations
Schaps, Stephen R.	• Electrical design • Nondestructive evaluation • Capacitance sensors
Schramm, Raymond E.	• Ultrasonic NDE of welds • Ultrasonic measurement of residual stress • Electromagnetic acoustic transducers
Shepherd, Dominique A.	• Charpy impact testing • Metallography and fractography • Thermomechanical processing
Shull, Peter J. (Until 6/90); Currently at Johns Hopkins Univ.	• Capacitive-array and eddy-current sensors • Electronics for EMATs • Nondestructive evaluation
Siewert, Thomas A.	• Welding metallurgy of steel • Gas—metal interactions during welding • Welding database management
Simon, Nancy J.	• Material properties at low temperatures • Database management of material properties • Handbook of material properties
Tobler, Ralph L.	• Fracture mechanics • Material properties at low temperatures • Low-temperature test standards
Walsh, Robert P.	• Mechanical properties at low temperatures • Mechanical test equipment • Large scale testing
Yukawa, Sumio	• Fracture mechanics • Codes and standards • Structural safety

TECHNICAL ACTIVITIES

PERFORMANCE

The Nondestructive Evaluation, Composite Materials, and Fracture Groups work together to detect damage in metals and composite materials and to assess the significance of the damage with respect to service performance.

Nondestructive Evaluation

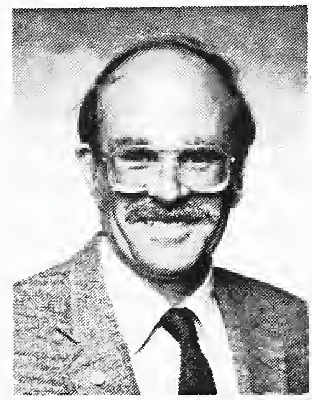

Alfred V. Clark, Jr.
Group Leader

Y. Berlinsky*, Y. Cohen**, M. Hirao∓, D. V. Mitrakovic∮, Stephen R. Schaps, R. E. Schramm, P. J. Shull (until 6/90)

Our Nondestructive Evaluation (NDE) group develops measurement methods and sensors for evaluating the quality and reliability of materials. We develop NDE techniques to characterize material properties, to detect and size defects, and to measure residual stresses in materials. Our research is transferred to industry for use in process control, quality assurance, and in-service inspection.

Representative accomplishments

- A prototype ultrasonic formability sensor was delivered to Ford for evaluation in their Dearborn stamping plant.

- Field trials were conducted on an ultrasonic system for roll-by inspection of railroad wheels.

Technical Highlights

During FY 90, the NDE Group was heavily involved in technology transfer efforts. A prototype ultrasonic instrument for measurement of steel sheet formability was developed jointly with researchers from Ford Motor Company. This device was delivered to Ford, where it is now in routine use.

---

* Guest researcher from ADA Rafael, Haifa, Israel.
** Guest researcher from the Nuclear Research Center, Negev, Israel.
∓ Guest researcher from Osaka University, Osaka Japan.
∮ Guest researcher from the University of Belgrade, Belgrade, Yugoslavia.

In a separate project, NDE Group members developed a system for roll-by inspection of railroad wheels. This system was subjected to three field tests at the Transportation Test Center (TTC). In the tests, locomotives and rolling stock passed over an ultrasonic transducer embedded in a rail. This system will be delivered to the American Association of Railroads after final modifications are made.

A third technology transfer effort involves design and construction of a system to receive laser-generated ultrasound. The system will be used for real-time evaluation of weld quality. Final tests are in progress to optimize system performance. Upon completion, the system will be delivered to the Idaho National Engineering Laboratory.

The ultrasonic transducers used in these systems all generate sound by an electromechanical transduction mechanism which does not require an intervening couplant or intimate contact with the specimen. They can work with a small (2-3 mm) air gap between transducer and specimen. Hence, they are ideally suited to applications where the material to be tested is in motion relative to the transducer.

Ultrasonic Instrument for Sheet Formability Measurement

The quality of sheet metal is a concern for both producers (steel companies) and users (for example, automotive companies). At present, there is no means of measuring steel formability in an on-line industrial setting, such as a steel rolling mill or an automotive body parts manufacturing facility. Research being performed by the NDE Group is being directed toward filling this gap.

The American Iron and Steel Institute (AISI) has expressed strong interest in this area of research. They have set goals regarding the accuracy of measurement of formability, and for the speed at which measurements need to be made. The NDE Group has structured its research towards meeting those goals.

In order to make reliable measurements on moving sheet, it is necessary to have a device which will move sheet specimens at speeds approximating those in a rolling mill. The Materials Reliability Division and the Ford Motor Company are cost-sharing the design and construction of a device which will be able to move sheet at controlled speeds up to 150 m/min. To date, four possible designs have been extensively studied, and a final selection made. When completed, the device will be delivered to NIST, and will be a unique measurement facility. It will be used as a "test bed" to determine what artifacts may occur when making measurements on rapidly moving sheet.

A two-fold approach is being used to improve the accuracy of formability measurement. Modelling is being done to try to predict formability from first principles. Here the inputs to the model are ultrasonic velocities measured at three different directions in the plane of the sheet. The model estimates the amount of preferred orientation (texture) of the single crystals in the sheet; the preferred orientation is a result of the thermomechanical processing of the sheet. Then the model predicts the plastic strain ratio (r-value), which is defined by $r \equiv \epsilon_\omega / \epsilon_t$. Here ϵ_ω and ϵ_t are, respectively, the strains measured in the width and thickness direction in a uniaxial tension specimen subjected to large plastic deformation.

The model is based on a simplified version of a theory developed at McGill University (Montreal, Canada). Progress in writing a computer code to implement the model has been greatly accelerated by collaboration with Professor M. Hirao (Osaka University), who is Japan's leading practitioner of the art of ultrasonic measurement of formability.

The second approach to improved accuracy is a careful study of means to improve ultrasonic velocity measurements. One parameter which causes uncertainty in these measurements is variation in distance (liftoff) between the ultrasonic transducers and the workpiece. The transducers generate ultrasound by electromechanical transduction; the effective circuit parameters for the transducers (inductance, resistance) consequently change with liftoff. This electrical impedance change gives rise to an apparent shift in the time between generation of sound waves at the transmitting transducer, and arrival of the wave at the receiving transducer.

A means to suppress this effect has been found, and will allow reliable measurements to be made over a range of liftoffs. This will be important when making measurements on moving sheet, where the transducers will be lifted off several millimeters in order not to interfere with the passage of rapidly moving material.

A study has been made of the influence of other variables on prediction of the r-value. Some of the results are illustrated in Figures 1 and 2. In Figure 1, sheets from one manufacturer and of one class of steel were used. One ultrasonic system was used to measure the average in-plane velocity, $\bar{V}$; one mechanical measurement system was used to measure the average r-value, $\bar{r}$. The spread is only about ±0.05, the goal AISI wishes to achieve. Figure 2 includes the data of Figure 1, plus: (a) steel from the same manufacturer, but measured by a second ultrasonic system, and (b) steel from a second manufacturer, measured with a different mechanical system (for $\bar{r}$), and a third ultrasonic system (for $\bar{V}$). It appears that the scatter in Figure 2 is worse, indicating that further work is necessary to refine the accuracy of measurements.

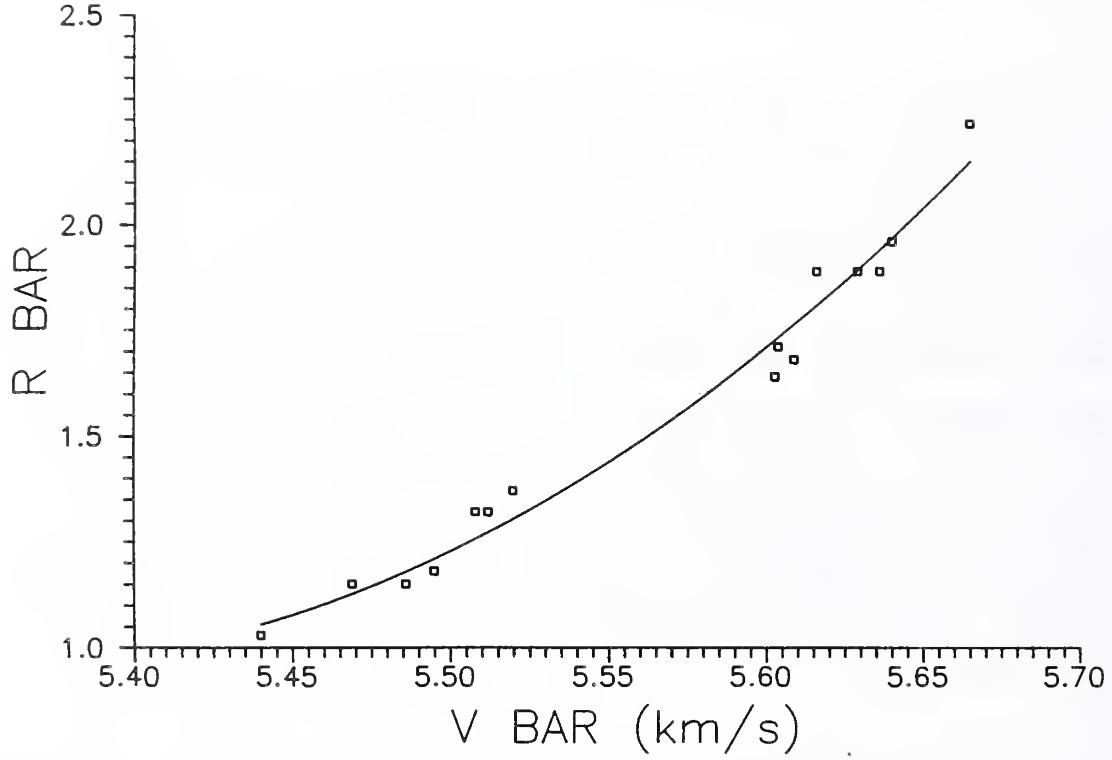

Figure 1. Measurements of the average plastic strain ratio, $\bar{r}$, versus the average in-plane velocity, $\bar{V}$, for a controlled experimental series.

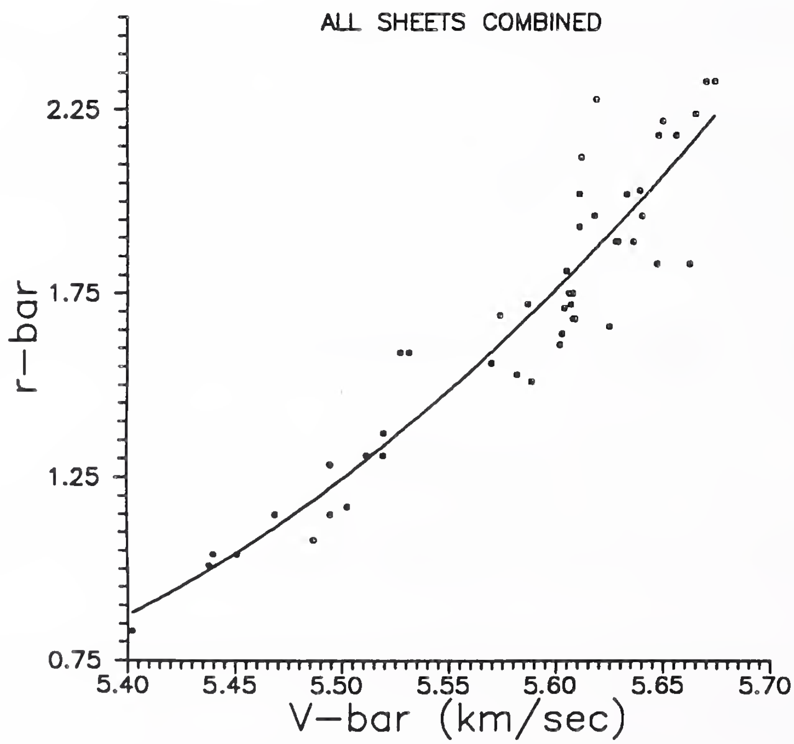

Figure 2. A summary of measurements of $\bar{r}$ and $\bar{V}$ from Figure 1 plus measurements obtained with different equipment on steels from a second manufacturer.

A prototype instrument for off-line r-value measurement has been developed jointly by researchers at NIST and Ford Motor Company. This device is shown in Figure 3. The rack of electronics on the right of the figure was developed at NIST in collaboration with a guest researcher (Prof. D.V. Mitrakovic, University of Belgrade, Yugoslavia). It consists of: a high-current pulser to drive the transmitting transducer; a low-noise, high gain amplifier to amplify the low-level signal picked up by the receiving transducer, a digital device to generate a STOP signal when a feature in the received waveform arrives. A commercial counter sits atop the electronics rack. It is started when the pulser delivers current and stopped by the digital device.

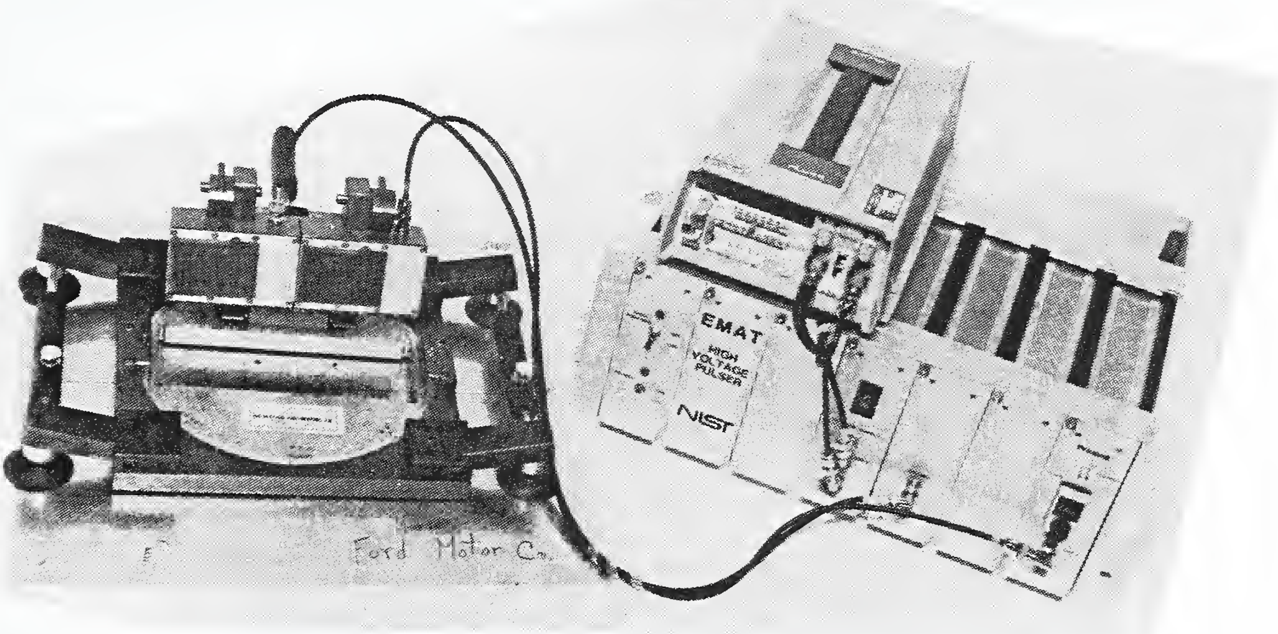

Figure 3. A prototype instrument for measuring r-values that is currently being evaluated at Ford's Dearborn stamping plant.

On the left side, a fixture is shown sitting on a sheet specimen. The fixture consists of a fixed platform, which supports a rotatable turntable. The turntable is rotated in 45° increments to allow velocity measurements to be made at different directions in the sheet. A slot is cut in the turntable to allow raising and lowering of the transducers. In Figure 3, the transducers are raised off the plate. The bottom of the transducer consists of serpentine coils, visible in the figure.

This device was delivered to Ford Motor Company. At present, it is being used in a joint project to obtain more mechanical and ultrasonic measurements on a wide variety of sheet specimens typically used in the manufacturer of automotive body parts. In FY 91, it is planned to improve this device by addition of improved electronics and transducers.

Ultrasonic Instruments for Railroad Wheel Safety

For several years, the Federal Railroad Administration has funded research to improve railroad wheel safety. On average, there are 33 derailments annually in the U.S. with annual economic loss estimated at $7 million. In addition, there is a significant safety hazard posed by toxic materials being transported by rail.

There are two primary causes of wheel failure leading to derailments: (1) cracks in the wheels, especially those originating in the wheel treads; (2) tensile stresses, which cause growth of cracks and subsequent failure. The NDE Group is developing two separate systems which will: detect defective wheels (with tread cracks) and measure the state of stress in the wheels.

Wheel Inspection System: A photograph of the ultrasonic system for roll-by inspection of railroad wheels is shown in Figure 4. The system consists of analog electronics, two transducers embedded in a rail section, digital electronics, and a computer for recording data.

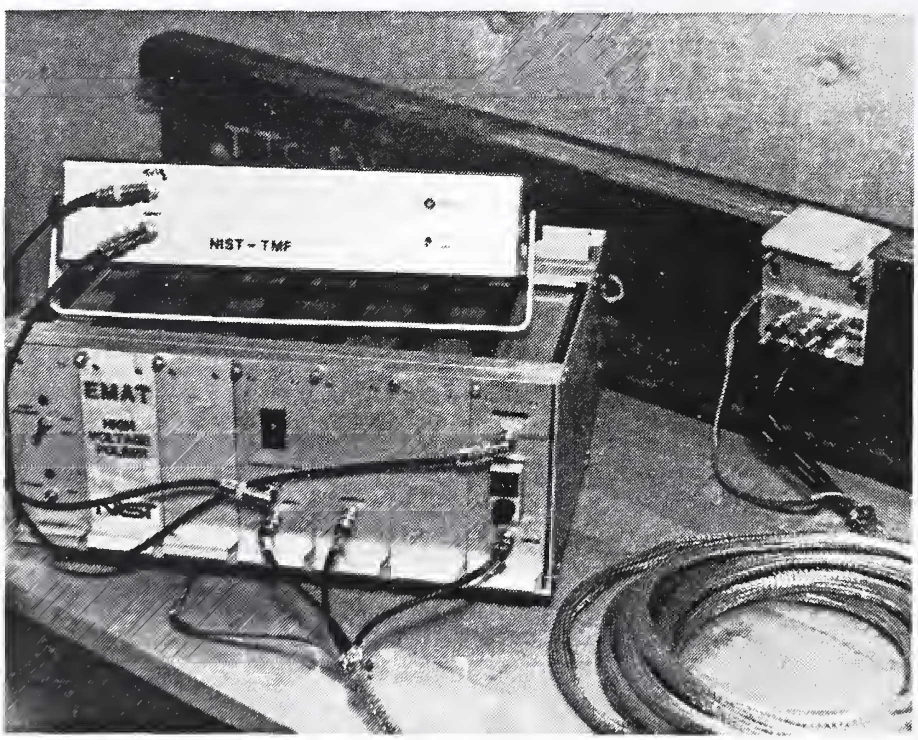

Figure 4. The ultrasonic system for roll-by inspection of railroad wheels.

In operation, the rail section is installed in existing tracks. Freight cars then pass over the rail section. As each wheel passes over the transducers, switches beneath the transducers are closed by the slight pressure exerted through a compliant foam (see Figure 5). The closing of the switches causes a trigger signal to be sent to a high-current pulser, which drives the transmitting transducer. This in turn generates a surface wave which travels around the wheel and reflects from any defects on the tread surface. These signals are detected by a second (receiving) transducer, placed directly beneath the transmitter. The signals are amplified by a low-noise amplifier, and are processed by the digital electronics. An algorithm is programmed into a microcontroller in these electronics; the algorithm decides whether a wheel is good, or needs to be removed from service. This information is displayed on a terminal within a minute (or less) after the passage of the train.

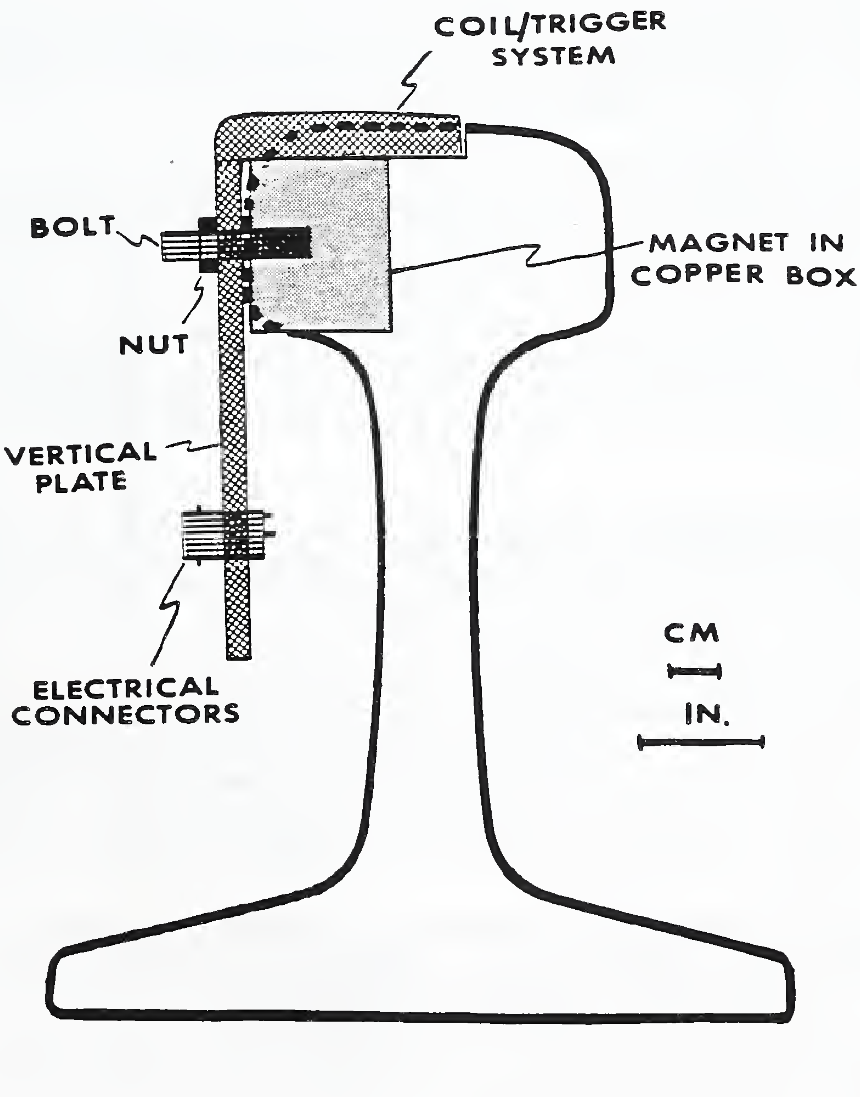

Figure 5. Rail section showing installation of the wheel-inspection transducer.

This complete system has been subjected to three field tests, using locomotives and rolling stock (freight cars). Tests were conducted at the Transportation Test Center (Pueblo, Colorado) in collaboration with researchers from the American Association of Railroads. Various tests assessed system performance in response to variables such as train speed, weight of rolling stock, electromagnetic interference, and types of wheel defects.

The first test revealed defects in the device which hold the transducers and trigger switches. This was redesigned and the improved version survived the passage of over 1500 wheels before failure. However, this improved device failed when subjected to passage of wheels with "false flanges", that is, raised ribs of metal on the wheel tread. A third version has been developed which can survive false flanges.

AAR personnel installed a variety of wheels on the rolling stock used in the tests. Some wheels were good, and others had previously been removed from service due to condemnable defects. In addition, a third class of wheels was installed, those with noncondemnable defects.

Tests revealed that, when all electronics performed correctly, the system could correctly identify both good and condemnable wheels. Thus, few "false alarms" (flagging good wheels as condemnable) and "false positives" (failure to identify bad wheels) should occur with the system.

In all tests, the analog electronics performed with complete reliability. Some defects in the digital processing were revealed by tests, and these have been corrected. Final documentation of all system components is proceeding, and the roll-by inspection system should be delivered to AAR in the fall of 1990.

<u>Residual Stress Measurement System</u>: When stress is applied to a metal, its sound velocity is changed. Typically, the change is small; for example, in steel a stress of 50 MPa causes a change in the of 4 parts in 10^4 in a shear wave propagating through the stressed region.

Unfortunately, other competing effects can cause an equally large velocity change. For example, in unstressed railroad wheel rims the difference of velocities of shear waves polarized in orthogonal directions (along a direction radially outward from the wheel center, and along a direction tangential to the wheel rim) are of the order of parts in 10^4. This circumstance makes it far more difficult to measure residual (as opposed to applied) stress in railroad wheels.

The cause of this difference in shear wave velocity (acoustic birefringence) is the preferred orientation of grains (single crystals) in the cast wheel as it cools. In general, the unstressed birefringence will vary with radial position, but will be approximately axisymmetric. Furthermore, even for the same radial position, the unstressed birefringence will vary somewhat from wheel to wheel.

To determine the effect of this inhomogeneity on residual stress measurements, the following experiments were conducted. Shear waves were propagated through the thickness of rim blocks cut out of actual wheels. The cutting process nominally removes any residual stress in the wheel, so the resulting acoustic birefringence, B_0, is due to the preferred orientation effect. On each rim block, B_0 was measured at 5 radial locations. A total population of 20 rim blocks (2 per wheel) were measured.

A typical result is shown in Figure 6, where all rimblocks are from wheels produced at a certain plant. A line has been fit to the data to show the radial gradient in B_0. The scatter about the line is primarily due to inhomogeneity in B_0 from wheel to wheel.

The effect of this scatter on residual stress measurements has been analyzed. Assuming that the data of Figure 6 are a true representation of the total wheel population, an error estimate can be made by taking the standard deviation of the difference between the linear fit and the data points. When converted into an equivalent stress error, this results in a stress uncertainty of approximately 35 MPa (5 ksi).

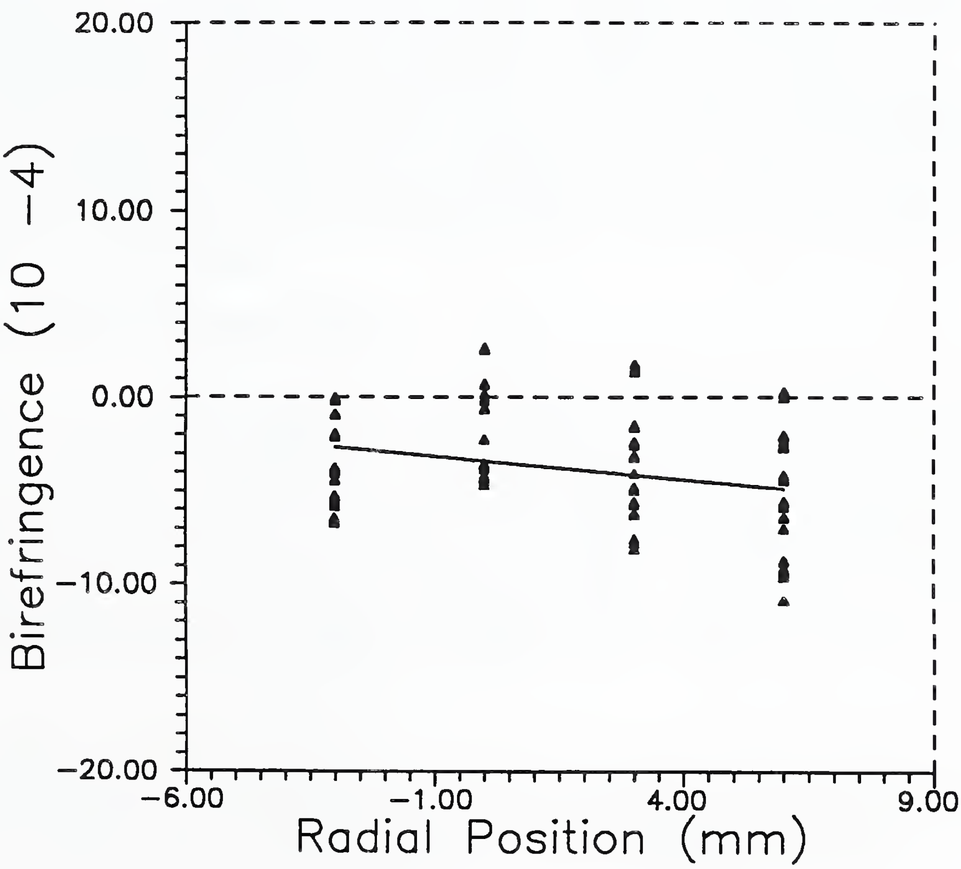

Figure 6. Acoustic birefringence as a function of radial position in wheel rims.

As part of this residual stress project, NIST is to deliver a complete system to AAR for further residual stress measurements. The system consists of pulsing and receiving electronics, a shear wave transducer, and a velocity measurement circuit. A transducer has recently been developed which has a signal-to-noise ratio several times higher than previous versions. The system is now undergoing final testing, and will be delivered in fall 1990.

Nondestructive Evaluation of Composite Materials

Christopher M. Fortunko
Research Leader

D.W. Fitting, V. K. Tewary*, L.J. Bond**, E. Jensen+, and M. Renken++

Our research in nondestructive evaluation (NDE) of composite materials is aimed at improved experimental methods for material-property characterization and flaw detection and sizing. In addition to a considerable experimental and special instrumentation-development activity, we are also developing theoretical models and computer-visualization aids, which are needed to establish model-based material-property and flaw characterization procedures. The Composites-NDE technical program also includes a broad range of university, other government agency, and industrial interactions.

Representative Accomplishments

(1) We designed and integrated a specialized high-power (10 kW), highly-linear (60-dB-plus), broad-band ultrasonic NDE system for inspection of a variety of advanced materials. This system, operating in the 60 kHz-60 MHz frequency region, enabled us to conduct experimental investigations of material conditions that are believed to reduce the interlaminar shear strength of thick marine composite materials: variations in fiber volume and porosity. In the future, we plan to exploit the unique low-frequency capabilities of our new ultrasonic measurement system to study fiber/resin interface conditions in polymer and metal-matrix composites.

---

* Visiting Scientist from Ohio State University, Columbus, Ohio
**NIST-supported Research Professor at University of Colorado at Boulder.
+ Co-op Student from Colorado School of Mines, Golden, Colorado.
++Co-op Student from Valparaiso University, Valparaiso, Indiana.

(2) We completed the integration of a unique air-coupled ultrasonic NDE system that is needed to evaluate materials that cannot be immersed in a coupling liquid. The system, which operates in the 0.25 kHz-2.5 MHz frequency region, has been used to conduct a number of material investigations of advanced high-temperature aerospace materials, automotive sheet-molding compounds (SMCs), wooden panels, and the like. We are currently working on a higher-frequency (25 MHz) gas-coupled system, which will be used to study electronic packaging materials.

(3) We formulated a general method for calculating the time responses of ultrasonic pulses in an anisotropic half space. The method is based on the use of a newly derived representation of a three-dimensional, time-dependent Green's function. The use of the new method significantly reduces computation times. We anticipate that the new method, which fully accounts for diffraction and discontinuities in a general anisotropic propagation medium, will lead to the design of significantly more sensitive ultrasonic inspection systems for composite materials.

(4) We developed and demonstrated the critical components of an ultrasonic inspection approach for very thick composite materials that are typically used in marine deep submergence applications. Currently, we are integrating a test-bed system that will demonstrate the technology. The new system uses linear arrays of very small, broadband ultrasonic transducers that are not sensitive to phase-front distortions caused by material inhomogeneities. To enhance the sensitivity to low-contrast features (for example, fiber-volume variations, fiber waviness, and porosity) the system will incorporate advanced image-processing using inputs from many transducers.

Improved Ultrasonic Instrumentation for Characterization of Thick Composite Materials

The NDE requirements of advanced composite materials cannot be met by using traditional ultrasonic instrumentation, particularly in the pulse-echo mode. Traditional ultrasonic-NDE instruments have been designed primarily to detect material flaws such as cracks and voids in metals. Although such flaws must still be detected and sized in composite materials, the instrumentation must also provide sensitivity to material-property variations. In particular, it is of considerable interest to characterize material parameters that do not exhibit high ultrasonic contrast: fiber-volume variations, fiber waviness, porosity, and fiber/matrix interface conditions.

The frequency ranges in which ultrasonic waves exhibit maximum sensitivity to a particular material property are well known. For example, variations in fiber/matrix interface conditions are known to affect the internal friction coefficient of a material. The internal friction generally increases linearly with frequency and can be measured at frequencies below 100 kHz. At higher frequencies, the ultrasonic attenuation is dominated by interlaminar scattering, which is sensitive to fiber-volume variations, and porosity.

Generally, fiber-volume measurements should be made in the 100 kHz-1 MHz frequency region, where the attenuation is proportional to the square of frequency, while porosity dominates the attenuation at frequencies above 1 MHz. Scattering from small pores is proportional to the volume of a pore and increases as the fourth power of frequency. Typically, the attenuation of an ultrasonic probing signal in a 50-mm-thick composite materials can vary from a fraction of a dB at 100 kHz to more than 80 dB at 2 MHz. Traditional ultrasonic-NDE generally cannot operate below 1 MHz and exhibit dynamic ranges of 30 dB.

To overcome the built-in performance limitations of traditional flaw-detection equipment, we have assembled a broadband, high-power ultrasonic measurement system that is specifically intended to meet the NDE requirements of very thick composite materials. A block diagram of our measurement system is shown in Figure 7. The system is intended to operate in the pulse-echo mode. In this mode, measurements of ultrasonic phase and group velocities, as well as attenuation as a function of frequency, can be made. All signal-processing and management functions are carried out digitally by a dedicated high-speed personal computer.

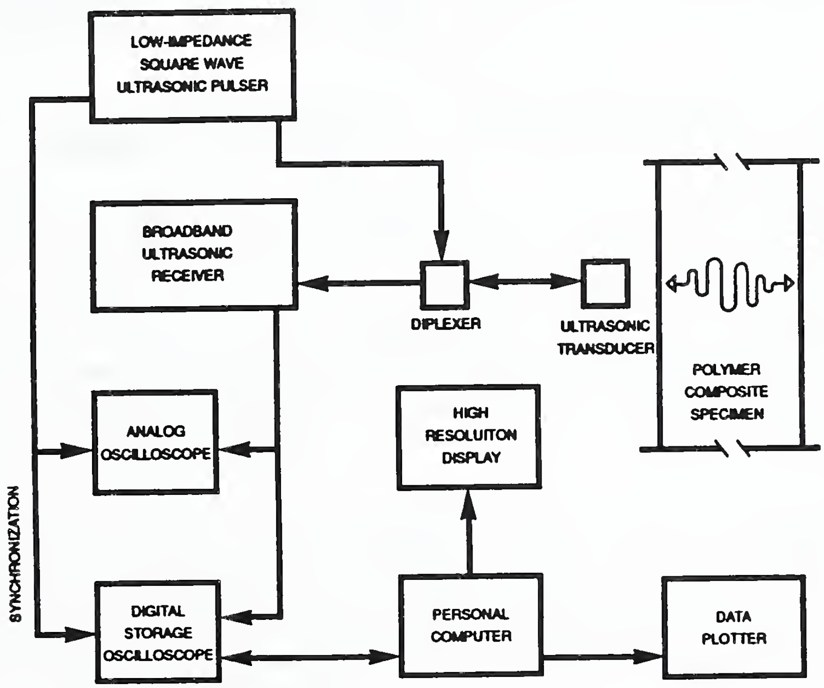

Figure 7. Ultrasonic system for NDE of thick composites.

The key performance attributes of our system are:

(1) Bandwidth: 60 kHz-60 MHz,
(2) Analog dynamic range: more than 60 dB,
(3) A/D converter resolution: more than 9 bits,
(4) Peak available pulse power: greater than 10 kW.

The longitudinal-wave velocity in a thick (45 mm) composite material made by a wet-filament winding process is shown as a function of location in Figure 8. The figure also shows plots of the thickness of the part and of the fiber content. The fiber content measurements are strongly correlated with the longitudinal-wave velocity measurements. Figure 9 shows a plot of the signal attenuation at 0.7 MHz. Also shown in this figure is a plot of the pore content. However, the two plots are not well correlated. We attribute this to the high elastic inhomogeneity present in this specimen. The elastic anisotropy causes phase-front distortions, which affect the conversion efficiencies of large-diameter ultrasonic transducers. Generally, elastic-wave velocity profiles correlate well with pore content.

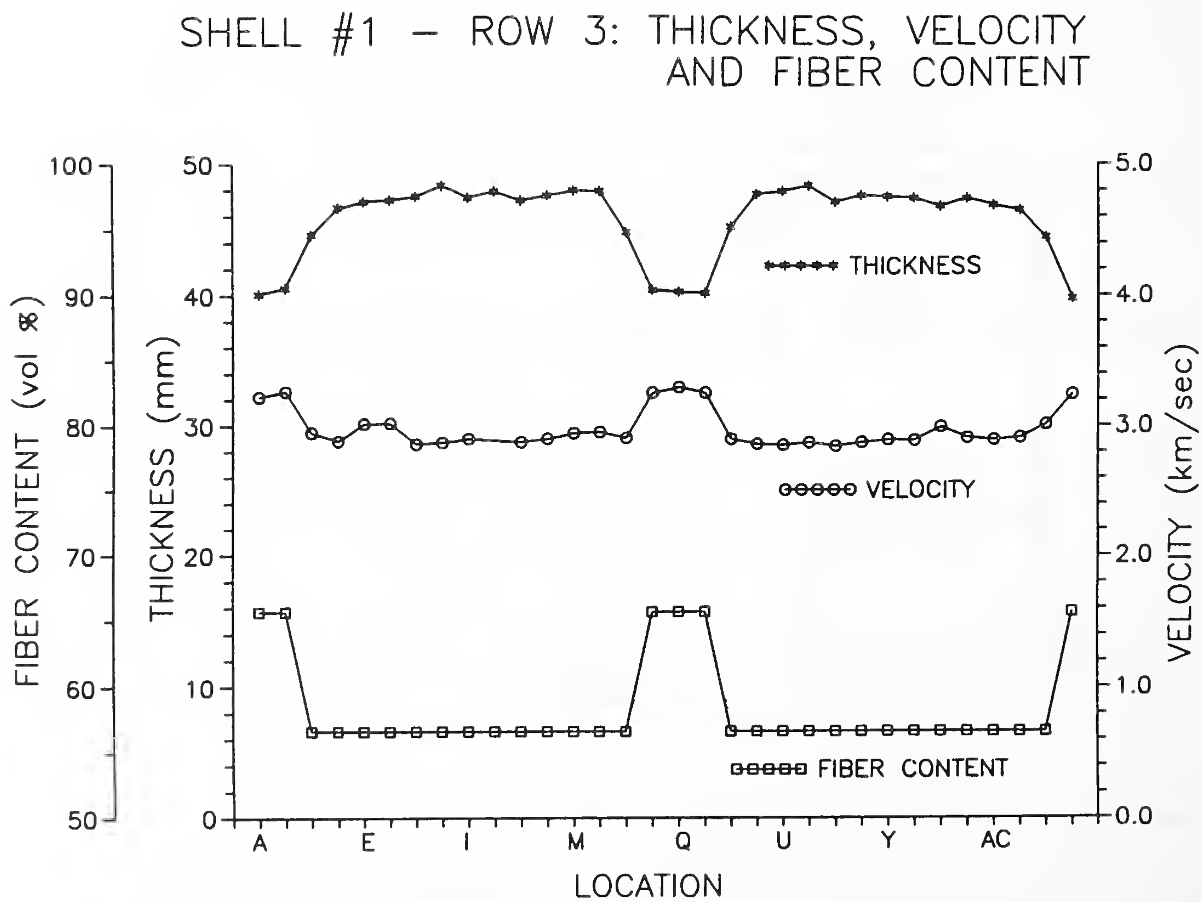

Figure 8. Elastic-wave velocity vs. thickness and fiber content for wet-filament wound structure.

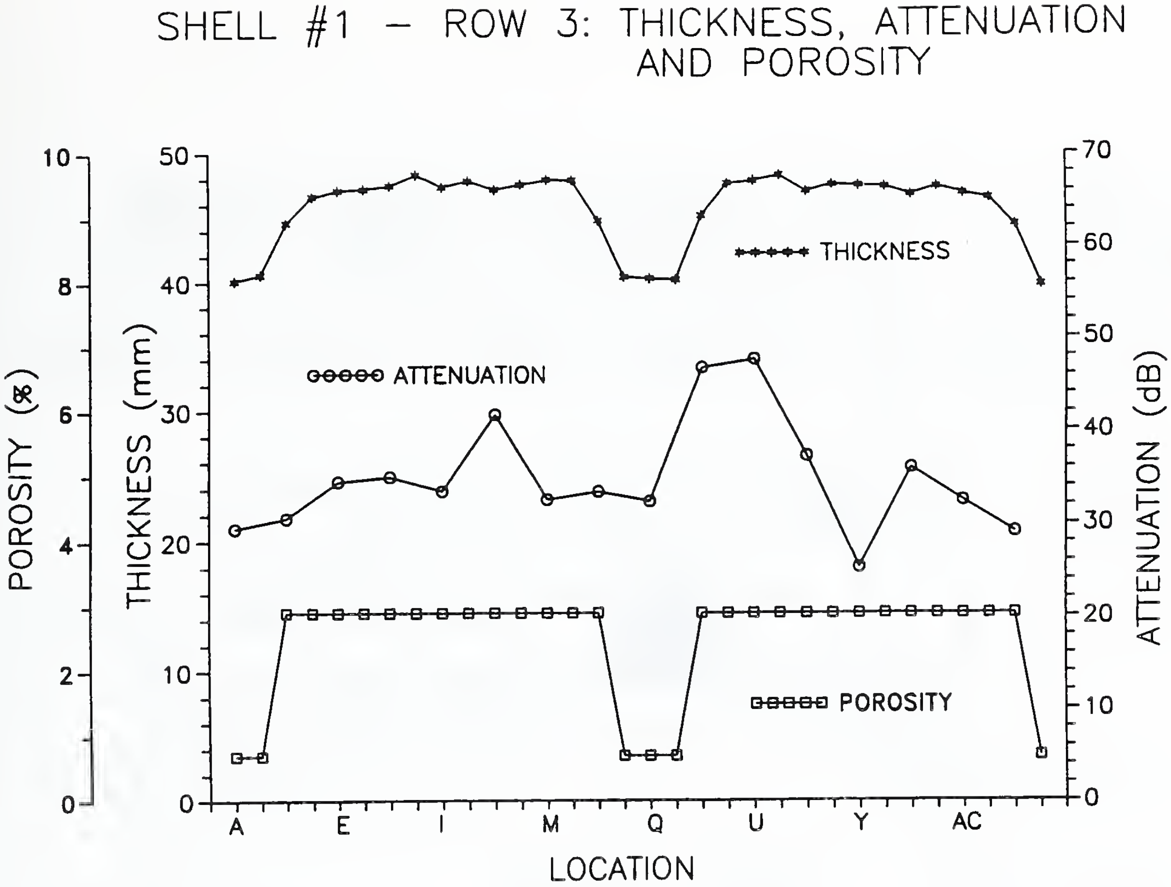

Figure 9. Ultrasonic attenuation vs. thickness and porosity for a wet-filament wound structure.

<u>Characterization of Composites Using Air-Coupled Ultrasonics</u>

The development of improved air-coupled ultrasonic systems is of interest because of potential applications in process control. Many materials, such as prepreg tape, advanced high-temperature composite materials, paper cannot be inspected at all by using traditional water-coupled systems or the newer laser-ultrasonic systems. However, such materials can be inspected by using air-coupled systems.

As a result of improvements in ultrasonic transducers and associated electronics, it is now possible to excite and detect ultrasonic waves in such materials by using air-coupled piezoelectric transducers operating at frequencies in the 400 kHz-2 MHz range. Systems operating at even higher frequencies (20 MHz and higher) may be in prospect. Such systems may be appropriate for inspecting high-density microchip carriers.

In the case of polymer composites, air-coupling enjoys one particular advantage over water coupling. The slow sound speed in air (300 m/s) insures efficient coupling to flexural waves in most thin composite materials. Such waves cannot generally be excited using water coupling, because the sound speed in water is typically 1100 m/s. Since flexural waves are generally slower than this value, efficient coupling cannot take place.

A 0.5 MHz air-coupled ultrasonic system has been designed and integrated at our laboratory to conduct ultrasonic studies of a variety of organic materials. A side view and the block diagram of the system are shown in Figures 10 and 11, respectively. The system can either be used to obtain ultrasonic raster scans ("C-scans") or polar scans of flat and circular specimens. The data can be interpreted to obtain flaw-content information (cracks, delaminations, etc.) or material-property information, including the elastic constants.

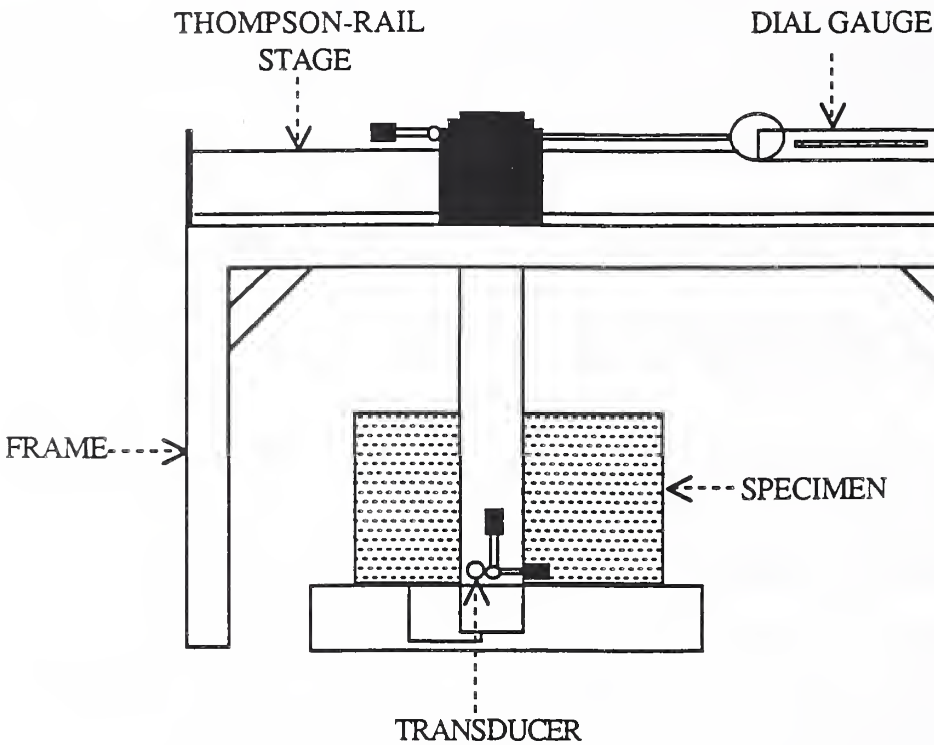

Figure 10. Air coupled ultrasonic system.

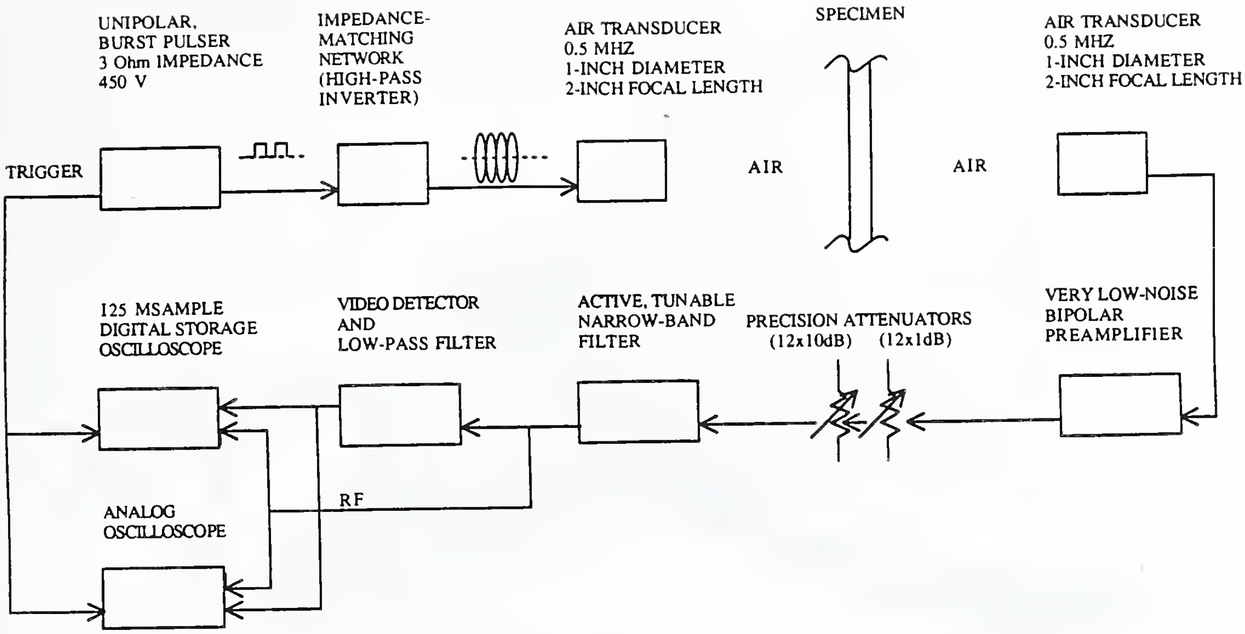

Figure 11. Block diagram of air-coupled ultrasonic system.

Theoretical Modeling

Propagation of elastic-wave interactions in anisotropic media has been the subject of intensive studies. However, most of the previous three dimensional treatments have been limited to the frequency-domain and infinite media. Although a number of time-dependent treatments were available, these were limited to two dimensions. For this reason, we undertook the development of a new representation of a three-dimensional, time-dependent Green's function.

The new method was first validated by comparison with a classical solution due to Pekeris and then applied to the calculation of scattering amplitudes from discontinuities in a general anisotropic medium. Two model discontinuities were selected: (1) a point scatterer and (2) a planar discontinuity.

The advantage of our method over methods based on finite-element approaches is that it allows three-dimensional, time-dependent wave-interaction calculations to be carried out using reasonably-large computational facilities. Currently, computation times of the order of several minutes on a NIST computer are required to obtain useful results. Figures 12 and 13 illustrate the time evolution of a pulse on the surface of a strongly-anisotropic cubic solid containing an interior point scatterer and a planar discontinuity. In these calculations, the value of the anisotropy parameter $(c_{11}-c_{12}-2c_{44})/c_{44}$ was taken to be 3. This parameter would be zero in an isotropic solid. The free-surface boundary condition was imposed at $x_1=0$. The applied force was taken to be a delta function at the origin, at t=0, and acting along the x_1 direction.

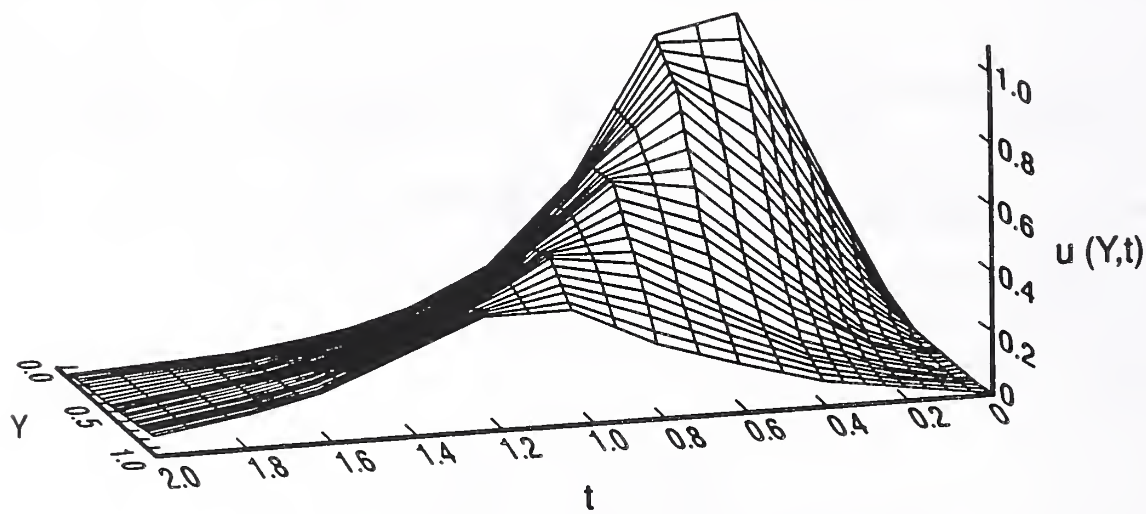

Figure 12. Time evolution of signal observed on the surface in the presence of interior point scatterer.

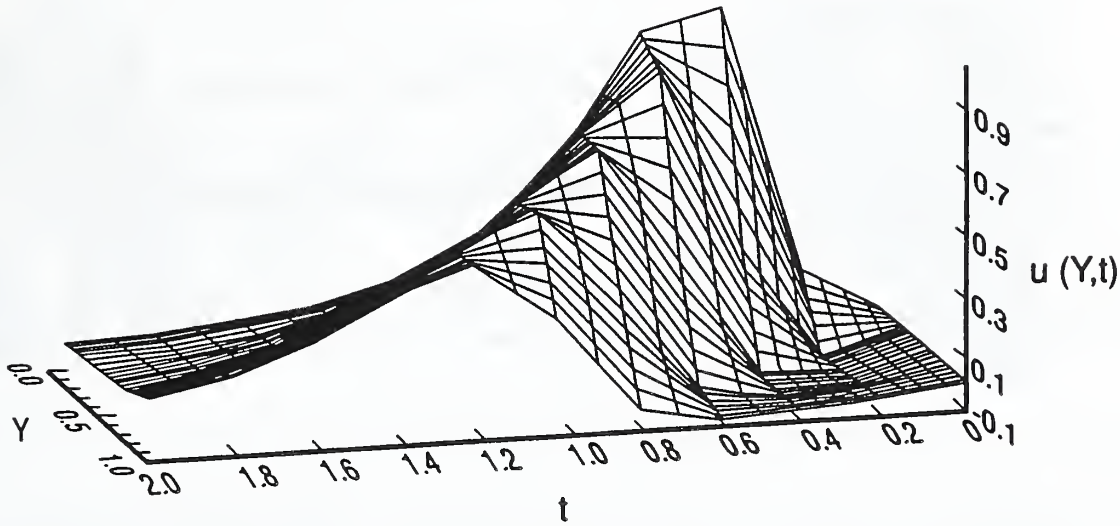

Figure 13. Time evolution of signal observed on the surface in the presence of internal planar discontinuity.

In the future, we plan to use our new Green's function representation to determine optimum transducer configurations for specific material anisotropies and specimen geometries. We also plan to use this representation to facilitate inversion of our experimental data to obtain material-property information: fiber/resin distribution, pore content, and flaw-size information.

Flexible Ultrasonic Transducer Arrays for Characterization of Thick Composite Materials

In response to NDE needs of the marine, aerospace, and off-shore industries, we are developing an ultrasonic NDE technology for very thick composite materials. Our approach overcomes one of the main barriers to inspectability in thick composite materials: phase-front distortions caused by strong elastic inhomogeneities. This is achieved through the use of flexible arrays of very small piezoelectric transducers.

Figure 14 illustrates our approach to the problem of NDE of thick marine composites. The transducer array is composed of a small number of high-power transmitting transducers, which introduce broadband (100 kHz-2 MHz) ultrasonic signals into the composite. The transmitted signals scatter from internal anomalies (delaminations, fiber wrinkles, cracks, and regions with anomalous pore content or fiber volume) and are detected by an array of very small receiver elements. Because the receiver elements are small in size (less than half wave at the highest frequency of the signal), they exhibit a wide field of view (FOV) and are generally insensitive to phase-front distortions caused by material inhomogeneities.

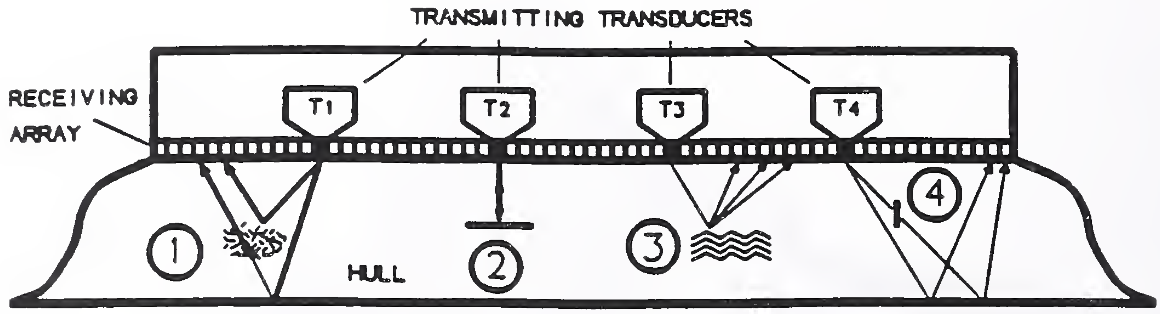

Figure 14. Transducer array for NDE of thick composites.

Figure 15 shows a typical ultrasonic radio-frequency (RF) waveform that can be processed by our system. In this case, the signal has traveled through approximately 50 mm of a wet-filament-wound marine composite material. The broadband nature of the signal and its high signal-to-noise ratio is evident.

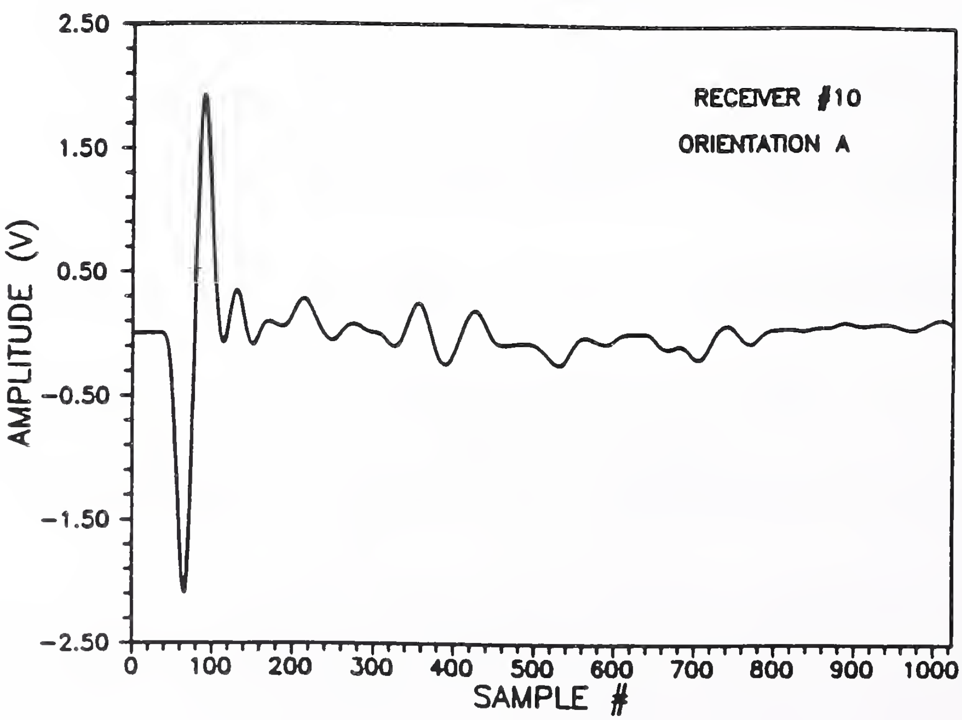

Figure 15. Typical ultrasonic wave form received after penetrating a 50 mm thick composite.

Fracture

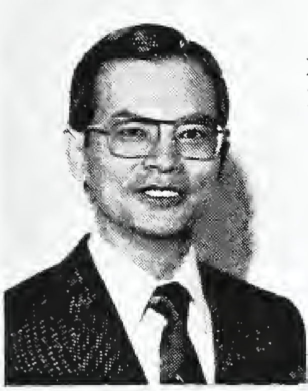

Ing-Hour Lin
Research Leader
Fracture Physics

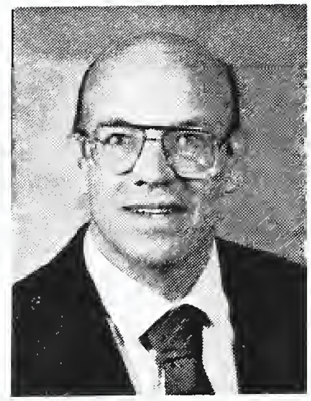

David T. Read
Research Leader
Fracture Mechanics

J.R. Berger, A.L. Preis*, M. Szanto**, V.K. Tewary+, R.M. Thomson, S. Yukawa

Our research in the mechanics and physics of fracture emphasizes advanced materials such as composite materials and electronic-packaging materials. In addition, we continue to study the fracture behavior of steels. In the case of composites, we are interested in damage mechanisms which are local events that deteriorate the strength and stiffness of composites, but do not necessarily trigger fracture. For electronic packaging, we are starting to develop experimental and analytical techniques for characterizing fracture behavior in thin films and multilayered materials.

Representative accomplishments

- To assess the significance of geometric irregularities in solder joints, automated finite element analysis procedures were developed to analyze joint geometry data obtained by x-ray laminography and optical NDE techniques. Results permit fitness-for-purpose evaluation of the significance of solder defects.

- Dislocation emission from a crack tip was modeled to gain an understanding of the phenomenon of brittle-to-ductile transition in silicon. The model includes the exiting and climbing components of the Burger's vector.

- The structure of a crack tip has been calculated in a covalent semiconductor. The calculation of crack opening near the tip accounts for the effect of electrons and the discrete atomistic nature of the solid.

---

* Co-op student from the University of Maryland.
** Guest researcher from the Nuclear Research Centre, Negev, Israel.
+ Visiting scientist from Ohio State University, Columbus, Ohio.

- A lattice statics approach has been used to calculate the structure of an interfacial crack in a composite material. Contrary to the nonphysical results of continuum calculations, the results indicate that the displacement and stress field are well behaved near the crack tip.

Mechanical Property Measurements on Thin Films

We are developing techniques to measure the mechanical properties of thin films as used in electronics devices. We think of this as a "testing machine on a chip," and call it a micromechanical properties study. The goal of the micromechanical properties study is to develop the methodology for measuring mechanical properties, starting with stress strain curves, for thin films under two special requirements: downward scalability and compatibility with electronic-packaging manufacturing processes. Downward scalability means that the micromechanical specimens can be scaled down repeatedly to smaller and smaller sizes, as the electronics industry scales down the feature size within their products. It also means that no manual machining and no handling of the specimen are done. The whole test device, including grips, force sensor, and specimen, is made using photolithography, and the specimen is tested in situ without ever touching it. Compatibility with electronic manufacturing processes is insured by using exactly those processes, specifically photolithography and wet and dry etching, to produce the test assembly.

Fitness-for-Purpose Assessment of Solder Joints

Solder joints are essential features of printed wiring boards (PWB), which are key building blocks in a wide variety of electronic devices from portable telephones to supercomputers. A new solder technology, called surface mount technology (SMT), makes much more efficient use of space on PWB than the previous through-hole technology, by using smaller components and mounting them closer together. This is accomplished by relying on the solder joint for mechanical attachment as well as electrical contact to the components. The SMT solder joint replaces long leads mounted in holes drilled through the PWB with shorter and smaller leads soldered to pads on the PWB. A variety of tests and inspections are now used to monitor SMT solder joints. However, the link between inspection results and device performance is currently a weak link. Improvement is being sought by using newly available commercial inspection hardware and recently developed commercial software for finite element mesh generation and finite element analysis to relate solder joint geometry to stress levels, and then eventually to the likelihood of failure. Within NIST, software has been developed to accept thousands of solder-joint surface point locations, find key features such as corners and cracks, and build finite element meshes around these features. Analysis of the resulting mesh gives the location and severity of high-stress points within the solder joint. Such points can initiate failure by, for example, initiating fatigue cracks, but the quantitative issues of how sharp the stress concentrations are and how high the stresses become are important.

Dislocation Modeling of Interfacial Fracture

Ing-Hour Lin served as a visiting scholar in materials science at Harvard University for one year starting September 1, 1989. The visit provided him the opportunity to redirect his dislocation and fracture physics research toward interface problems, particularly those associated with electronic packaging. Working with Professor James R. Rice and his research group at the Division of Applied Science Division, Harvard University, a simple model for dislocation emission from a crack tip be developed to gain an understanding of the phenomenon of brittle-to-ductile transition. In this two-dimensional model, the total energy per length of crack front is composed of three terms, respectively, due to the mismatch deformation, the applied load, and the elastic self-energy of dislocations. Analytic formulas were derived for the dislocation incubation zone size and stress intensity factors for emission in terms of dislocation configuration and angles between slip and cleavage planes. We have work under way to explore the different effects of mixed mode loading and dislocation configuration on dislocation emission from a crack tip in silicon. The interaction between dislocations and an interfacial crack in bimaterials is also being studied to understand the plasticity and interfacial toughness for thin films deposited on substrates and fibers in composites.

Deformation and Fracture of Thin Films

Reliability in electronic devices requires better understanding of strain relaxation in semiconductor heterostructures. We study straining processes and residual stresses in thin films due to mismatching of lattice constants and thermal expansion coefficients between thin films and substrates. Our work focuses on the injection of dislocations and cracks in the multilayer structure because mechanisms and critical stresses corresponding to nucleation processes of defects have not been completely identified and solved.

Atomistic Theory of Fracture of Covalent Semiconductors

In cooperation with K. Masudo-Jindo, a guest researcher from the Tokyo Institute of Technology, the structure of a crack tip has been calculated in a covalent semiconductor which accounts for the effect of the electrons and the discrete atomistic nature of the solid. Using the lattice Green's function approach and LCAO (linear combination of atomic orbitals) electron theory, we investigated the atomistic configuration and lattice trapping of cracks in Si. The LCAO electron theory coupled to second order perturbation theory (SOP) has been used to derive explicit expressions for the bond breaking nonlinear forces between Si atoms. We calculate the cracked lattice Green's functions for a crack on the (111) plane and lying in the (110) direction. With the nonlinear forces acting in a cohesive region near the crack tips, the crack structure is then calculated. The calculated structure possesses a crack opening at the Griffith load which should allow penetration of typical external molecules to the crack tip at the Griffith loading.

The calculations give valuable information about the crack opening near the tip and crack growth rate as influenced by the quantum effects in the solid. This study forms a basis for further work on chemical effects on the crack growth and failure of semiconductors. The quantum effects are likely to be important near the crack tip in semiconductors and are not normally included in the usual continuum fracture mechanics.

Interfacial Fracture in Composite Materials

The continuum fracture mechanics predicts an obviously unphysical result that the surfaces of an interfacial crack in composite materials interpenetrate each other; that is, an interfacial crack closes onto itself. Moreover, the stress near the interfacial crack tip is predicted to be strongly oscillatory which makes it difficult for interpretation of crack growth data in composite materials. The results mentioend above are artifacts of the continuum theory arising from its nondispersive nature. In this study, a lattice statics approach has been used to calculate the structure of an interfacial crack. A method for calculating lattice statics Green's function was developed for a composite solid containing a plane interface. The method involves creation of two half-space lattices containing free surfaces and then joining them to form a composite. The two half-space lattices may have different structures or may be of the same type but joined at different orientations to form a grain boundary interface. The composite Green's function is then used to calculate the lattice statics Green's function for the composite containing an interfacial crack and the displacement field due to an applied external force.

The method, which is quite general, has been applied only to a simple model composite formed by two simple cubic lattices with nearest neighbor interactions. The results indicate that the displacement as well as the stress field are well behaved near the crack. The lattice statics formulation will be particularly useful for studying failure of electronic packaging where interfacial fracture between semiconductor and oxide layers may be influenced mainly by electronic and atomistic structure of the solids.

Dynamic Fracture Mechanics

In cooperation with J.W. Dally and R.J. Sanford of the University of Maryland, we have investigated the suitability of strain measurements for the analysis of dynamic fracture experiments. Specifically, an analysis method was developed which made use of the spatial variations in strains recorded by a series of rosette gages positioned above the crack path. Following an overdetermined analysis of the strains, both propagation toughness and crack-tip position could be determined. The analysis methodology was applied to large-scale dynamic fracture tests in cooperation with R.J. Fields and R. de Wit of the Metallurgy Division.

It is necessary to specify which gages may be included in an overdetermined analysis based on the position of the gage relative to the propagating crack tip. Information from gages remote from the current crack-tip position may introduce error into the analysis if they lie outside the region where the three-parameter model adequately describes the strain field. We studied the extent of validity of the three-parameter model to arrive at criteria for inclusion or exclusion of gages from the analysis.

To assess the validity of the three-parameter strain field model, a series of finite element analyses was conducted to determine the series coefficients in a large order expansion of the strain field. Through knowledge of the higher order (nonsingular) terms, we examined the error over a reasonably sized area between strain calculated from a three-parameter model and a strain calculated using a large order model. We study this error by simply choosing a point in the field, calculating the strain at this point using both three- and large-parameter models, and comparing the two strain values. As we vary the position of the point throughout the field, we can begin to see where strain gages provide information usable in the spatially overdetermined analysis procedure. By performing this analysis for a variety of crack lengths, we determine the gage inclusion/exclusion criteria.

The Cryogenic Materials and Physical Properties Groups investigate the behavior of materials at low temperature and measure and model the properties of advanced materials, including structural alloys, conductors, composites, ceramics, and superconductors.

Cryogenic Materials

Richard P. Reed*
Group Leader

A. Bussiba**, E. S. Drexler, J. D. McColskey, P. T. Purtscher, R. L. Santoyo, N. J. Simon, R. L. Tobler, R. P. Walsh

We study the mechanical, physical, and metallurgical properties of materials in the temperature range 4 to 295 K. Goals of our research are the characterization and development of metals, alloys, and composites; the development of testing procedures and standards; and the collection and evaluation of material properties data.

Three major programs were funded by other agencies during the past year: (1) the Department of Energy continued to sponsor the development of materials technology to design and build superconducting magnets for fusion-energy systems; (2) the Air Force sponsored a program to evaluate aluminum-lithium alloys for cryogenic tankage in the Advanced Launch System; and (3) the Strategic Defense Initiative funded an evaluation of fiberglass struts for use in the superconducting magnetic energy storage system. We have expertise in and unique facilities for measuring tensile, shear, creep, and fatigue properties at very low temperatures. We contribute to design and safety assessments, and consult on material selection and properties for a wide range of cryogenic projects.

---

* R.P. Reed retired in March 1990 after 33 years of Federal service.
**Guest researcher from the Nuclear Research Centre, Negev, Israel.

Representative accomplishments

- A short-crack simulation test was developed and used to measure the fatigue crack growth threshold of cryogenic alloys at 4 K.

- The oxygen compatibility of aluminum-lithium alloys was shown to be satisfactory for use of these alloys for liquid oxygen tankage.

- Fiberglass composites were evaluated at room and cryogenic temperatures for use as thermal-isolation struts for a superconducting magnetic energy storage system.

- The physical and mechanical properties of beryllium-copper and phosphor-bronze alloys from over 250 documents were added to our database on cryogenic materials.

Oxygen Compatibility of Aluminum-Lithium Alloys

The purpose of the Air Force-sponsored oxygen-compatibility program was to assess the relative compatibility with liquid and gaseous oxygen of high-strength Al—Li alloys and alloy 2219 for use in Advanced Launch System (ALS) cryogenic tanks. Program objectives were: (1) to provide well-characterized specimens of state-of-the-art commercial alloys for LOX (liquid oxygen) and GOX (gaseous oxygen) measurements at either of the qualified NASA test laboratories, Marshall Space Flight Center (MSFC) and White Sands Test Facility (WSTF); (2) to study the roles of intrinsic material variables, such as fracture properties, chemistry, and second phase particles, on ignition characteristics; and (3) to assess the extrinsic test variables, such as impact energy, pressure, temperature, and specimen size, orientation, and specimen location (within the specimen cup or holder) on reaction tendencies.

Al—Li alloys 8090-T3 and 2090-T81, and Al alloy 2219 (tempers T851 and T37) were tested for compatibility with liquid oxygen using pressurized mechanical-impact apparatuses at MSFC and WSTF. Specimens and data from tests at Santa Susana Field Laboratory (SSFL), Rocketdyne, on alloy 2090-T81 were supplied by ALCOA. Pressurized mechanical-impact data on alloy WL049-T351 were produced by WSTF. In addition, WSTF conducted open-cup mechanical-impact and promoted-combustion tests on all of these alloys. In following studies, selected tempers of alloys 8090, 2090, WL049, and 2219 were tested in modified open-cup and pressurized mechanical-impact equipment at WSTF. Drop height (potential energy), pressure, and environment (liquid oxygen, LOX and gaseous oxygen, GOX) were varied in these tests. Additional promoted-combustion tests were also conducted at WSTF.

Reactions, ranging in size from those that could be observed with the naked eye to those that required use of the scanning electron microscope (SEM), were identified in all alloys. Those that require little or no magnifying power to view are labeled macroreactions; those that require the use of optical microscopy or SEM are called microreactions. Al—Li alloys had more macroreactions than 2219; 2219 had more, or an equivalent number of microreactions, than each of the Al—Li alloys. Al—Li alloys were superior to 2219 in flammability in the presence of GOX, as measured in the promoted-combustion tests. Therefore, within the ability of the current tests to discern relative compatibility and flammability with LOX and GOX, the Al—Li alloys and 2219 must be judged equally acceptable for ALS cryogenic tankage.

The mechanical-impact test imparts significant deformation (absorbed) energy to the Al-alloy specimens. Axial compression, radial shear, and circumferential tensile (hoop) stresses are all of the order of magnitude required to fracture the specimen. From these large stresses, most specimens crack internally or fracture (split) inwardly from the perimeter. The minimum absorbed energy needed to induce splitting (tensile failure) in the specimen has been compared to the minimum absorbed energy needed to induce reactions in the specimen. The minimum energy to induce fracture was less than, or equal to, that required to induce reactions. Therefore, mechanical failure will precede, or usually be attendant with, reactions in oxygen environments.

The discovery that reactions with oxygen occur over a large range of sizes emphasizes an inherent ambiguity in the definition of a reaction in mechanical-impact tests. Current practice of accepting only visual observations leads to inconsistencies (reactions may be overlooked and their observation depends on proper lighting conditions). The size of reactions observed in these tests has not been correlated with in-service performance. Furthermore, we suggest ten modifications to the current NASA NHB 8060.1B standard for mechanical-impact tests in LOX or GOX; these changes would reduce the large disparity in test procedures that exists among laboratories that conduct these tests. In summary, the definition of a reaction is arbitrary and modifications are needed to ensure closer conformance of testing procedures. For these reasons, it is recommended that the current open-cup and pressurized mechanical-impact, oxygen-compatibility tests not be used as a qualification test for alloys in aerospace applications.

Evaluation of a Superconductor Conduit Alloy

High-field superconducting magnets use A15-type superconductors in austenitic alloy conduit sheaths. The conduit sheaths protect the superconductor cables and also contain the liquid helium coolant at 4 K. The cable components and conduit are heated together during fabrication at temperatures around 700°C. This heat treatment reacts the Nb and Sn elements to produce the superconducting compound Nb_3Sn. It also ages the conduit and adversely affects its mechanical properties.

The mechanical properties of austenitic stainless steels that are proposed as conduit materials are degraded during aging by sensitization (carbide precipitation). Precipitation of $M_{23}C_6$ carbides on grain boundaries is particularly deleterious. One method to combat this problem is to add small amounts of Nb to retard the rate of carbide formation.

A conduit for superconductor cables was tested to evaluate its suitability for International Thermonuclear Experimental Reactor magnets at liquid helium temperature. The conduit material, JK1, is a 316LN alloy modified by the addition of 0.05% Nb. Tension, fatigue, and fracture toughness were measured. A short crack simulation technique was used to measure fatigue crack growth rates and thresholds. At 4 K, the alloy's yield strength after heat treatment exceeds the targeted 1200 MPa, but its toughness (J_{Ic} = 40 kJ/m^2 for the T-L orientation) is lower than desired or expected from alloy development studies. Metallurgical differences between rolled plate and formed conduit, or between research grade and commercial processing could account for the difference in toughness.

Fatigue Crack Growth Thresholds

Fatigue crack growth rates and threshold stress intensity factors are relevant to superconducting magnet design because they can be used to predict safe operating conditions and lifetimes. Typically, fatigue crack growth rates (da/dN) are plotted versus the stress intensity factor range (ΔK); the data on log-log coordinates define a curve that may be divided into three stages: very low rates approaching threshold values, intermediate rates of growth, and high rates approaching instability.

In Stage I (low ΔK), the crack growth rates diminish and approach an asymptote called the threshold, ΔK_{Th}. Measurements near threshold are time consuming and difficult to perform, so few data are available in this stage. In Stage II (intermediate ΔK), the measurements are easier and can be completed in relatively short time; consequently, the database for cryogenic materials in Stage II is larger than in the other stages. In Stage III (high ΔK), the crack growth rates for materials accelerates as ΔK approaches the upper critical limit of fracture toughness. This third stage is seldom studied because the crack growth rates are too high for practical applications.

Measurements of fatigue crack growth rate are reported for five austenitic stainless steels at room and cryogenic temperatures (76 or 4 K). The alloys evaluated in this study were AISI 316, 316LN, 304L, 304LN, and 304HN. The rate measurements span the range 10^{-6} to 10^{-10} m/cycle, and threshold stress intensity factors are identified at 10^{-10} m/cycle. The apparent thresholds for the five steels range between 6.5 and 10.5 MPa·m$^{1/2}$ and vary slightly with material and temperature. The effective thresholds (that is, the apparent thresholds corrected for crack closure) are uniformly lower than the apparent thresholds and range between 4 and 7 MPa·m$^{1/2}$. At 4 K, the thresholds increase moderately with yield strength which ranges from 610 to 1270 MPa for these alloys.

Technology Transfer Highlights

The results of our materials research is transferred to the cryogenics community through annual reports and workshops, compilation of materials property data and dissemination in the form of Handbook pages, and the development of test standards. Highlights for 1990 are summarized below:

- The Twelfth Annual Cryogenic Structural Materials Workshop was organized; it was held October 11–12, 1989 in Vail, Colorado.

- "Materials Studies for Magnetic Fusion Energy Applications – XIII", (NISTIR 90-3944, 382 pages, 1990, editors R.L. Tobler and R.P. Reed) was prepared, published, and distributed.

- Handbook pages on the cryogenic tensile, elastic, electromagnetic, fatigue, and thermal properties of C17000–C17510 beryllium-copper were prepared and distributed.

- Handbook pages on C50500–C52400 phosphor-bronze tensile, elastic, fatigue, electromagnetic, and thermal properties are in preparation. Documents (over 250) have been acquired, and preliminary data sets extracted and analyzed. Equations relating yield strength, tensile strength, and elongation to cold work, temperature, Sn content, and grain size between 4 K and room temperature have been developed from the database. Further analysis of other properties is in progress. These alloys are used as stabilizers for Nb_2Sn superconducting cable.

- The cryogenic database for AISI 316LN has been updated with data acquired since the AISI 316 handbook pages were prepared in 1982. A preliminary report on this database was presented at the ITER Specialists Meeting on Magnet Materials in Garching in February 1990. Alloy 316LN is a prime candidate for use in thick sections in the toroidal field coils in the ITER design.

- Nine drafts of a proposed standard 4-K tensile test procedure were written and submitted for review at domestic and international workshops. The ninth draft has been formally submitted to ASTM, and is two-thirds of the way through the balloting process required to establish a new standard.

- At ASTM's request, the sixth draft of a proposed standard for 4-K fracture toughness testing was rewritten in the form of an annex for ASTM Method E 813-89; the annex was submitted to ASTM to begin due process for standardization.

- Research on the problems of Charpy impact testing at 4 K was conducted. NIST, the Massachusetts Institute of Technology, and the Japan Atomic Energy Research Institute cooperated to produce three research papers on this subject. On the basis of this work, balloting has begun at ASTM on a revision of the notched bar impact test standard, Method E 23-88.

Physical Properties

Hassel Ledbetter
Research Leader

T. Ashizawa†, D. Balzar°, M. Földeáki‡, S.A. Kim, M. Lei*, S.-H. Lin§

Our research emphasizes measurements and modeling of elastic constants and related physical properties of metals, alloys, composites, ceramics, and the new oxide superconductors. For many studies, the temperatures range between 295 high-T_c and 4 K. The elastic constants, which relate deformation to stress, sustain our interest because they relate to fundamental solid-state phenomena: interatomic potentials, equations of state, and phonon spectra. Furthermore, thermodynamics links elastic constants with specific heat, thermal expansivity, atomic volume, and the Debye temperature.

Representative accomplishments

- We began a large study of the effect of mechanical deformation on the low-temperature elastic constants and magnetic susceptibility of f.c.c. Fe–Cr–Ni–Mn alloys. These materials show a low-temperature paramagnetic– antiferromagnetic phase transition. Initial results show that deformation smears out the elastic-constant transition. Deformation-induced changes in magnetic susceptibility are small, but measurable.

---

† Visiting scientist from Hitachi Chemical Company, Japan.
° Visiting scientist from Physics Department, Faculty of Metallurgy, University of Zagreb, Yugoslavia.
‡ Visiting scientist from Institute for Materials Testing and Quality Control, Budapest.
* Graduate student from Institute of Metal Research, Shenyang, China.
§ Graduate student from Physics Department, Tsinghua University, Beijing, China.

- We made a thorough measurement–modeling study on the elastic properties of (polyether) etherketone (PEEK) reinforced with alumina–silica fibers. We found good measurement–modeling agreement. The study required calculating the elastic constants of the γ–Al_2O_3/SiO_2 fibers. In turn, this required estimating the unknown γ–Al_2O_3 elastic constants. This effort also succeeded.

- We began a large effort to measure both the phase and group ultrasonic-wave velocities in high-T_c metal-oxide superconductors. Some basic models of superconductivity require a difference in these two velocities. Initial results on Eu–Ba–Cu–O show only a small difference, both above and below the normal–superconducting transition temperature. (On this study, we worked with C. Fortunko.)

Austenitic steels

Our current efforts comprise three topics

1. Chemical-composition effects on physical-property changes at the low-temperature paramagnetic–antiferromagnetic phase transition

2. Mechanical-deformation effects on magnetic susceptibility

3. Electron-concentration effects on physical properties

Under the second topic, we completed the following study. We studied Fe–Mn–Cr alloys with the basic chemical composition (18% Mn, 18% Cr, balance Fe) with different additions of microalloying elements, especially C and N. We studied them both as-quenched (from about 1200°C) and cold-worked state (38% for the low-N/high-C specimen, and 52.4% for the high-N/low-C specimen). For all cases, the magnetization curves were linear, showing no traces of ferromagnetic impurities or minority phases. An antiferromagnetic–paramagnetic transition occurs near 240 K in all cases. For the high-N/low-C specimen, deformation effect is small, corresponding to a decrease of the transformation temperature by about 5 K and a slight broadening of the $\chi(T)$ peak. For the low-N/high-C specimen, the broadening of the peak after deformation is larger, and the decrease of the transformation temperature equals 15 K. The susceptibility of the deformed specimen shows a smaller decrease below the transition temperature.

We also studied the effect of annealing on the magnetic susceptibility. After annealing, both specimens show nonlinear magnetization curves over the entire studied temperature range. This tendency is largest at low temperatures in the deformed annealed specimen. The antiferromagnetic–paramagnetic transition can be revealed only by detailed analysis of the magnetization processes.

Future research plans include identification of the metallurgical and magnetic nature of these phases. Because the application temperature of these steels may be in the range of heat applied for annealing (650°C), the practical importance of these results cannot be overlooked.

Composites

Here, we completed three measurement–modeling studies

1. Tungsten particles in a copper matrix

2. Gamma-alumina–silica fibers in a polyether-etherketone matrix

3. Silicon–carbide whiskers in an aluminum-oxide matrix

Summaries of these three research efforts are as follows.

Using a megohertz (MHz)-frequency ultrasonic method, we measured the elastic constants of a composite consisting of seventy-volume-percent tungsten particles in a copper matrix. We report the Young, shear, and bulk moduli, and the Poisson ratio. Tungsten is much stiffer than copper: the Young-modulus ratio equals 410/129 = 3.2. Thus, from a linear rule of mixture, we expected large departures, which we found. (The Poisson ratio comes close to a linear rule of mixture.) Unexpectedly, we found a substantial elastic anisotropy: eighteen percent on the shear modulus. To model the system, we used a scattered-plane-wave ensemble-average approach. For the four elastic constants listed above, we found reasonable model–measurement agreement, 1–7 percent for the averaged-over-direction measurements. Assuming oblate-spheroidal (c/a = 0.5) particles improves the agreement: 2 percent or less for the four cases.

Polymers reinforced with alumina fibers provide many desirable properties. These include higher elastic stiffness (the alumina/glass Young-modulus ratio equals 210 GPa/76 GPa = 2.7); higher fiber elastic modulus usually means higher fatigue resistance; a thermoplastic matrix, polyether-ether-ketone (PEEK), usually also raises fatigue resistance; a thermoplastic material provides processing–fabrication advantages over a thermoset material; low thermal-conductivity-to-mass ratio. Using both a MHz-frequency pulse-echo method and a kHz-frequency resonance method, we measured the elastic constants of a uniaxial-fiber-reinforced plastic-matrix composite: 0.52-volume-fraction of aluminum-oxide fibers in a polyether-ether-ketone matrix. Measurements agree well with a model calculation using the ensemble average of scattered plane waves. Getting good agreement required assuming elastically anisotropic fibers. Cooling to 4 K shows that C_{11} increases 30% and C_{44} increases 34%. (Coordinate system: x_3 along fibers, x_1 through-plate direction, x_2 third orthogonal direction, in plate.) Both C_{11} and C_{44} vary smoothly with temperature; below about 100 K, both show an irregular stiffening.

Using MHz-frequency ultrasonic methods, we measured the ambient-temperature elastic constants of a ceramic–ceramic composite: randomly oriented silicon-carbide whiskers in an aluminum-oxide matrix. We considered two whisker volume fractions: 0.15 and 0.30. The materials showed little dependence of elastic properties on direction, indicating a nearly random fiber arrangement. All the elastic constants — Young, shear, bulk moduli and Poisson ratio — agree well with a model calculation. The model uses the ensemble average of scattered plane waves. To do the modeling, we estimated the five α-SiC(4H) elastic constants, which were previously unknown.

Superconductors

We focus principally on five classes of metal-oxide superconductors:

1. La–M–Cu–O M = Ca, Sr, Ba
2. Nd–Ce–Cu–O
3. Pr–Ce–Cu–O
4. Bi–Sr–Ca–Cu–O
5. Y–Ba–Cu–O

Our studies involve five principal ingredients:

1. Characterization

   1.1. microstructure
   1.2. magnetic susceptibility
   1.3. x-ray diffraction

2. Elastic-constant measurements between 295 and 4 K

3. Modeling, principally the bulk moduli by a Madelung-energy model

4. Relationships between elastic properties and other physical properties

   4.1. Debye temperature
   4.2. electron–phonon parameter, λ

5. For polycrystals, corrections to the void-free state

For the current fiscal year, we want to mention two principal studies.

Ultrasonic-wave studies of the new high-T_c oxide superconductors. A review published in an IUTAM proceedings. We highlight studies that began in spring 1987 on high-critical-temperature oxide superconductors. The superconducting systems include La–Sr–Cu–O, Y–Ba–Cu–O, and Bi–Sr–Ca–Cu–O. In the latter system, T_c approaches 110 K. Most existing studies focus on sound velocities and elastic constants between ambient temperature and 4 K. Because almost all studies focus on polycrystalline sintered ceramics, I consider effects of voids on sound velocity. Some specimens contain more than fifty-percent voids. Thus, large effective-physical-property changes occur, especially if the voids assume nonspherical shapes. The relatively low Poisson ratios (near 0.21) shown by the superconductors suggest that their interatomic bonding resembles that in perovskites such as $BaTiO_3$ and $SrTiO_3$ and in some, but not all, other metal oxides. Temperature hysteresis of sound velocities suggests a phase transition similar to that occurring in relaxor ferroelectrics. Sound velocity provides an especially sensitive probe of this transition, more sensitive than other physical properties such as electrical resistivity or specific heat. Because many believe that strong anharmonic effects occur in these materials, we consider the Grüneisen parameter, which we can obtain either from sound velocities or their pressure derivatives.

Elastic constants and Debye temperature of $Y_1Ba_2Cu_3O_x$: effect of oxygen content. Intended for Physica C. Using ultrasonic methods, we measured the elastic constants of polycrystalline $Y_1Ba_2Cu_3O_x$ between 295 and 4 K. For a single specimen, using vacuum annealing and oxygen annealing, we varied the oxygen content in four steps from $x = 6.2$ to $x = 6.9$. Elastic stiffnesses that depend mainly on shear modes increase monotonically with increasing oxygen content. Stiffnesses that depend on dilatation modes increase up to about $x = 6.7$ and then decrease. The elastic Debye temperature, which depends mainly on shear modes, increases monotonically, in agreement with the specific-heat Debye temperature. An ionic-model calculation for the bulk modulus and Debye temperature predicts a monotonic increase for both. We conjecture that the irregular oxygen-content dependence of the dilatation-mode-related elastic constants arises from changes in copper—oxygen valences.

Some other oxide-superconductor efforts this year include the following:

1. phase-velocity and group-velocity measurements (with C. Fortunko)

2. calculation of cation and anion valences using known crystal structure, ion positions, interionic distances, and coordination numbers

3. low-temperature measurements on several materials listed above

4. detailed x-ray-diffraction studies of La—M—Cu—O system with view toward possible future Rietveld-refinement analysis.

Finally, we want to mention a new activity: working with division 724, we try to fabricate our own metal-oxide bulk superconductors. Acquiring good specimens for physical-property studies is a sine qua non that presents real obstacles to research. Work under way includes synthesizing Y—Ba—Cu—O/Ag and Bi—Sr—Ca—Cu—O, both from acetate-solution mixtures. These specimens will also provide a chance to study weak-link behavior and flux-pinning associated with grain boundaries.

MATERIALS PROCESSING

The Welding and Thermomechanical Processing Groups measure and model the physical and metallurgical changes that occur during material processing, such as metal transfer in arc welding, recrystallization, and phase transformation. These changes affect the quality, microstructures, properties, and performance of metals.

Welding

Thomas A. Siewert
Group Leader

M. W. Austin, P. Heald*, R. B. Madigan, C. N. McCowan, M. A. Mornis*, T. P. Quinn, D. A. Shepherd, D. P. Vigliotti

The Welding Group conducts materials research to improve the quality, reliability and safety of welded materials. Our goals include the development of sensors, measurement procedures, and controls that can automate the production of consistent, high quality welds. We also develop weld metals with improved tolerance for defects. A specific goal for a Navy-sponsored program is to develop a more fundamental understanding of the process of droplet transfer across the arc, then incorporate this information into an intelligent weld controller that improves the quality and efficiency of welding.

The Welding Group is also responsible for radiology NDE and the OSRM Charpy V-notch calibration program.

Representative accomplishments

- Through-the-arc sensing has been shown to detect contact tip wear, one of the problems that has limited the automation of gas metal arc welding. We are broadening the study to other contact tip alloys and welding filler materials, so that a general model may be developed.

---

* Graduate students, Colorado School of Mines, Golden, Colorado

- The NIST diagram for predicting ferrite content in stainless steel welds was adopted by the American Society of Mechanical Engineers for use in the Boiler and Pressure Vessel Code.

- This group has completed its first year as the source of Charpy V-notch reference specimens and calibration services, for world-wide certification of these machines to the ASTM (E23) Standard.

Arc Physics

Our laboratory capabilities have been upgraded substantially. Our high speed video system (60 Hz in the full frame mode and 300 Hz in the partial frame mode) has been replaced by a substantially faster system (1000 Hz in the full frame mode and 6000 Hz in the partial frame mode). It is combined with a laser vision system that back-lights the arc, while filtering the high intensity light generated by the arc. This upgrade will allow much better resolution of individual droplet transfer events during spray transfer.

The data acquisition system has been improved with the replacement of the computer control system by one having a 25-MHz processor, integral math coprocessor, and high-speed cache. The analog-to-digital board was replaced with a 100 kHz bipolar version, for better resolution of differential signals.

The new equipment is being used in a joint program with the U.S. Navy and Babcock and Wilcox, to design and build a welding system that demonstrates advanced sensor technology and other system improvements. Our contributions are an ultrasonic weld flaw sensor and an arc sensor that uses the weld voltage and current signals. In this program, we have demonstrated the ability of the welding current signals to reveal wear of the contact tip. Figure 16 illustrates how the standard deviation of the current signal increases as the contact-tube diameter increases. The figure shows the data from three separate tests at each tip diameter. The envelope of the data has sufficient slope (and a sufficiently narrow scatter) in the initial wear region to allow real-time monitoring of the tip condition.

The arc physics laboratory continues to generate cooperative programs. Three students from the Colorado School of Mines are using the laboratory for further studies in determining tip wear, droplet transfer mode, and developing alternative sensor technology. We expect another student to start in the first quarter of 1991.

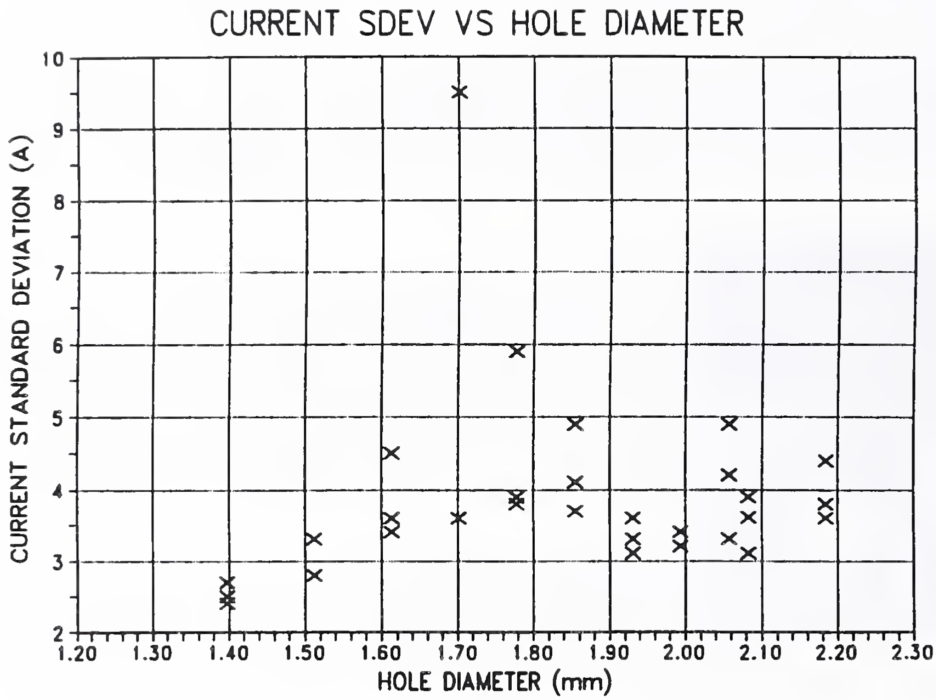

Figure 16. Current changes as a function of contact tip wear, which is simulated by enlarging the inside diameter of the tube (hole).

<u>Charpy V-notch Calibration Program</u>

The Charpy impact test is a small-scale laboratory and industrial fracture experiment that uses a pendulum-type drop hammer and a centimeter-size material specimen to measure the ductile or brittle behavior of steel. It is the most widely used standard for predicting the fracture behavior of steel because of its simplicity and low cost.

The calibration program begins with NIST furnishing a series of V-notched reference specimens that are broken on a customers' machine. Fracture energy and other test data are entered on a questionnaire and returned with the fractured specimens. The data are analyzed and acceptable machines receive a letter indicating conformance. If problems are found, a letter is sent indicating the probable source of the discrepancy.

We have completed our first full year as the administrators of this program. It was transferred from the U.S. Army Material Technology Laboratory in Watertown Massachusetts to NIST last Summer, and we have concentrated our efforts on providing a smooth transition. The program responsibility is divided between two groups within NIST, with sales of the reference materials by the Office of Standard Reference Materials and evaluation of the returned data and specimens by the Materials Reliability Division. We have performed these evaluation services for about 1000 machines, from around the world, during the past year.

Two specimen energy ranges (near 17 and 98 J) continue to be available, and a super high energy range (near 160 J) was added this year. During the next year, we plan to add an intermediate energy range (near 55 J) to align the certification procedure with changes being balloted within the ASTM Committee (E28) responsible for the standard. We are also evaluating new materials for more consistent values within the existing energy ranges. An emerging problem is the growth in the use of an International Standards Organization specification which uses a different striker design. We are studying ways to bring the two standards into agreement.

Real-time Radioscopy

This program is developing standards to support the change from conventional film-based radiography to the more efficient and faster filmless (video screen based) radioscopy. Current image quality indicators, which were designed for use in film-based systems, must be repositioned between exposures and are not suitable for the translation and rotation modes possible with radioscopy systems.

We have developed new image quality indicator designs, with one and two degrees of rotational symmetry, to meet the need of standards for images produced with this new technology. This design is easy to locate and the center provides a measure of the contrast resolution of the system. Figure 17 is a gray-level plot showing the good resolution of a 2% difference in thickness between the center of the IQI and the adjacent absorber plate. These devices are now being evaluated in several round robins.

Other technological developments are occurring in the areas of finer resolution x-ray tube designs and laminography (the production of two-dimensional slices through a three-dimensional structure). Here, we are also developing special standards. For the finer resolution possible with smaller focal spots, we have inverted the concept of a pinhole camera. Preliminary measurements indicate an ability to go to much finer resolutions than with the drilled hole design, while avoiding the problems of alignment and poor photon density.

We have a joint program with the U.S. Army and the NIST Office of Nondestructive Evaluation to develop standards for laminographic systems for inspection of solder joints on printed circuit boards. We have developed a new image quality indicator design to measure the Z-dimension resolution of such systems. In addition we are developing a board to calibrate the measurements of such a system by reference to primary dimensional measurements.

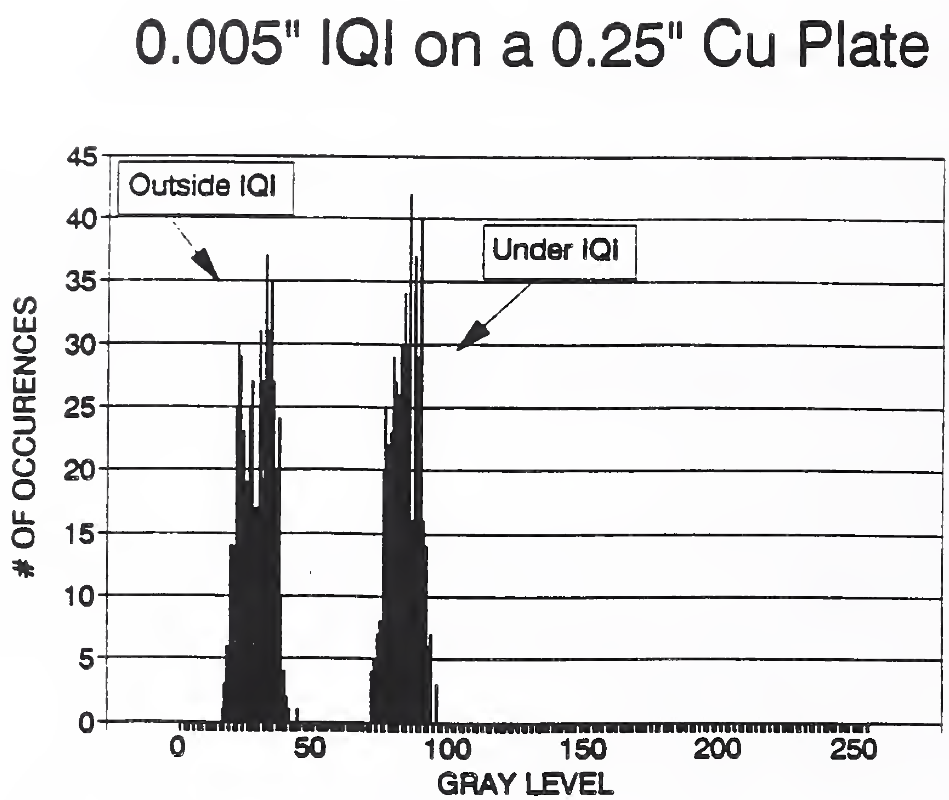

Figure 17. Gray level plot showing the resolution of a new image quality indicator (IQI).

Radiography Standards for Aluminum Welds

In a joint program with the U.S. Army and Image Quality Incorporated, we are developing aluminum welds with known flaws. We are producing a matrix of welds in different thicknesses of plate (3 and 12 mm), different densities of flaws, and different flaw sizes and shapes. The welds are being radiographed for evaluation by an ASTM committee (E07). Eventually the radiographs will become available as ASTM standards, while the welds will be reserved for further study or reradiography in the future. Preliminary evaluations indicate about half of the desired weld flaw categories have been produced, with the rest to be completed in the next year.

Stainless Steel

In support of Department of Energy cryogenic applications, we have been evaluating various stainless steel electrodes, and cataloging the properties of their welds. Three different electrode types or ranges were investigated this year.

In support of the design of the Compact Ignition Tokamak by Princeton Plasma Physics Laboratory, we evaluated a series of shielded metal arc electrodes that were expected to reveal the appropriate composition for joining type 316LN or type 21Cr-6Ni-9Mn stainless steel plates for this high-strength

76 K design. These electrodes were variations on a type 385 (20Cr-25Ni) gas metal arc electrode which was found to develop an exceptional good combination of strength and toughness last year. Preliminary assessment of these compositions reveals the expected strength, but insufficient toughness. The cause is still being determined, but seems to be related to the inclusion content.

Another experiment was based on nitrogen additions (through the shielding gas) to a gas metal arc electrode version of the type 385 composition. We found the best combination of strength and toughness that has been measured in our laboratory for a weld at 4 K. In support of the Princeton program, we measured the mechanical properties at 76 K, and found a yield strength near 780 MPa and a Charpy V-notch absorbed energy near 140 J, again the best combination of these properties which we have measured. A special heat (containing the desired levels of nitrogen and manganese) has been ordered for evaluation next year.

The final experiment was the addition of nitrogen to a type 316LN gas metal arc electrode. Although the microstructure contained ferrite, the solidification mode indicated primary austenitic solidification. The strength met the desired goals, but the toughness was less than that desired. We attribute the low toughness in this weld to a fracture mode that progressed through brittle interdendritic regions.

The ferrite prediction diagram which we reported last year, has been reviewed and adopted by the American Society of Mechanical Engineer's Boiler and Pressure Vessel Code and will be included in the Fall 1990 Addendum. It has also been submitted to the International Institute of Welding for use as an international standard.

Analysis of Fluxes

In support of standards development and control procedures within the U.S. Navy, we are evaluating techniques for the analysis of welding fluxes. Our goal is to identify a method whereby we can control the flux composition and predict welding problems such as poor bead shape or hydrogen cracking.

For many welding processes, the flux is an integral part of the electrode, and it is evaluated during qualification testing. Submerged arc welding is an exception; the electrode and flux can be combined in an arbitrary manner. Thus, qualification of one electrode-flux combination can not necessarily be transferred to another. This program is investigating the use of new evaluation techniques.

Thermomechanical Processing

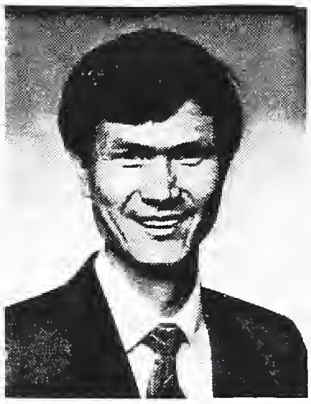

Yi-Wen Cheng
Research Leader

R. Kuziak*, A. Tomer**

Research in thermomechanical processing uses a deformation-processing simulator built at NIST. We study the metallurgical changes that occur in steels during forging and subsequent cooling. By controlling the deformation-temperature schedules, the cooling after forging, and the subsequent tempering treatment, we are striving to achieve optimum strength and toughness in directly cooled and directly quenched forging steels.

Representative Accomplishments

- Equations have been developed to generalize the effects of temperature on flow behavior of a microalloyed forging steel, and to predict the austenite grain size during hot working.

- Procedures using a personal computer were established to determine true stress-vs.-true strain curves, phase-transformation temperatures during continuous cooling, strain rate, and cooling rate after a TMP simulation experiment.

Technical Highlights

Microalloyed (MA) medium-carbon forging steels have been introduced to the automobile industry as economical substitutions for some quenched-and-tempered (Q-T) grades. Cost reduction is the driving force for developing MA steels, which are to be used in the as-cooled condition. Cost reduction is realized through the elimination of heat treatment, straightening, stress relieving, and improved machinability. These MA steels can achieve tensile

---

* Guest researcher from the Institute of Ferrous Metallurgy, Gliwice, Poland
**Guest researcher from the Nuclear Research Centre, Negev, Israel

strengths comparable to those of Q-T steels, but with inferior impact properties. Research to improve the impact properties of the directly cooled MA steels is increasing. Several approaches to raising the toughness while lowering the ductile-to-brittle transition temperature have been cited in the literature [1–3]. These include: (1) lowering the carbon content from 0.5% to 0.35 or 0.25%; (2) lowering the reheating temperature and the finish-forging temperature to control the austenite (γ) grain size; (3) adding Ti (to produce TiN particles) to control γ grain size; (4) modifying the steel chemistry, such as increasing Mn or Si content; (5) controlling MnS inclusions to increase intragranular ferrite nucleation; and (6) producing low-carbon bainitic steels.

Lowering the deformation (finish-forging) temperature will change the γ grain morphology, which will, in turn, influence the austenite-to-ferrite transformation kinetics and the final microstructure. Lowering the deformation temperature will also increase the flow resistance of the steel and reduce the forgeability. The goal of the present study is to investigate the effects of deformation temperature on the transformation kinetics of a MA SAE 1141 steel in terms of continuous-cooling transformation (CCT) diagrams, and to determine the high-temperature flow characteristics of the steel. Attempts were also made to generalize the effects of deformation temperature on flow stress, and the recrystallization of γ after deformation.

Continuous-cooling transformation study

Continuous-cooling transformation characteristics following different deformation schedules were established for microalloyed SAE 1141 forging steel. We have measured the effects of hot deformation on the phase-transformation kinetics under continuous cooling condition. We found that deformation above A_{r3} and below nonrecrystallization temperatures not only enhances the formation of ferrite but also refines the ferrite grains substantially. CCT diagrams for SAE 1141 steel with and without prior deformation are shown in Figures 18 and 19.

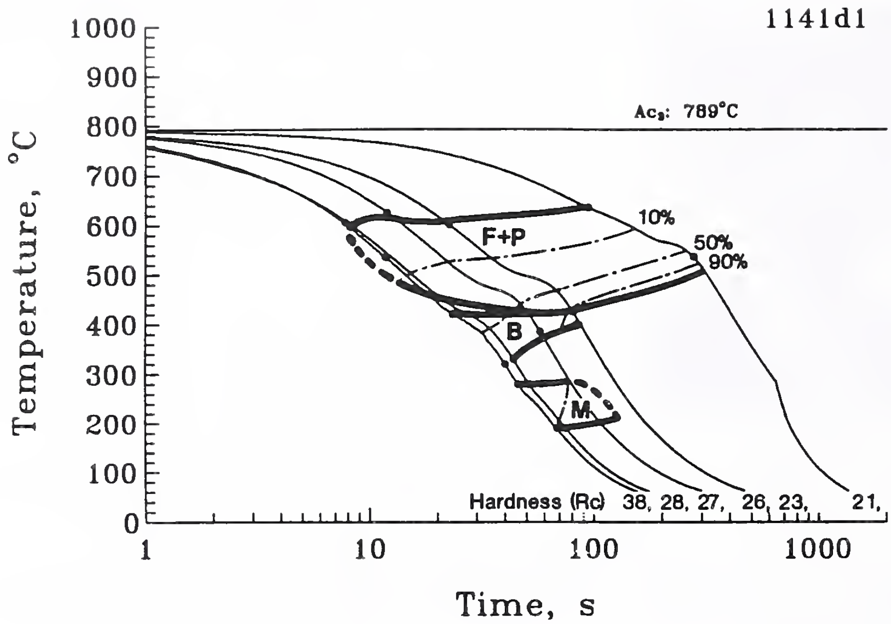

Figure 18. The CCT diagram of the microalloyed SAE 1141 steel after reheated to 1218°C and compressed 50% at 900°C. F: ferrite; P: pearlite; B: bainite; M: martensite.

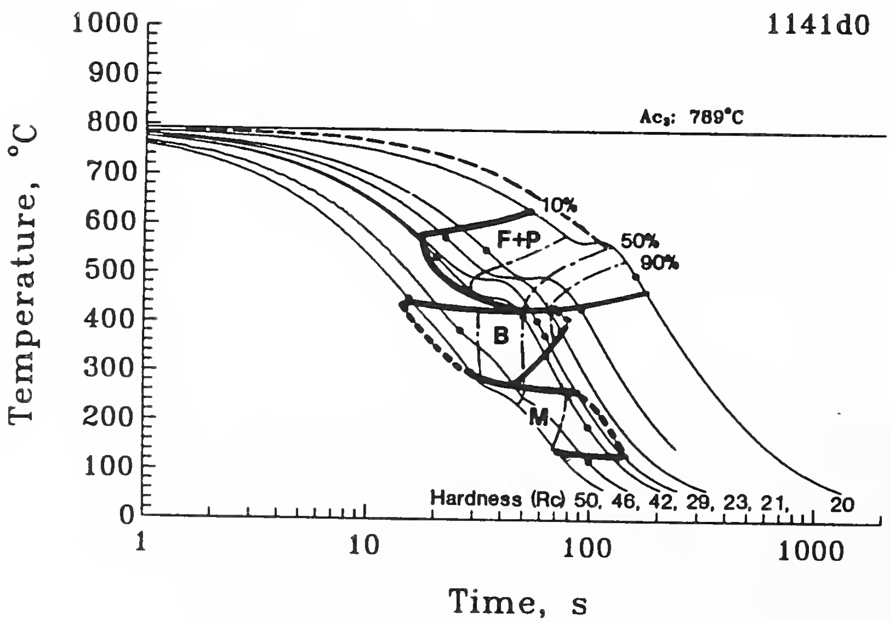

Figure 19. The CCT diagram of the microalloyed SAE 1141 steel after reheated to 1218°C. F: ferrite; P: pearlite; B: bainite; M: martensite.

Characterization of high-temperature high-strain rate flow property

High-temperature high-strain rate flow characteristics are important in modeling forging and plate rolling. As part of the TMP research, we characterize the flow curves of steels at high temperatures under constant true strain rate. We found that for microalloyed SAE 1141 forging steel the temperature dependence of flow stress at constant strain and strain rate followed the equation, $\sigma = C \cdot \exp(Q/RT)$, where σ is the flow stress, C is a constant, Q is an activation energy for plastic flow, R is the universal gas constant, and T is the testing temperature.

Determination of recrystallized austenite grain size after deformation

Fine austenite grain sizes are a prerequisite for obtaining fine ferrite grains that simultaneously increase strength and improve toughness. During hot working, the developing of recrystallized austenite grain sizes followed the equation, $d_{rex} = C \cdot d_0^{m} \epsilon^{n}$, where d_{rex} is the recrystallized austenite grain diameter, d_0 is the austenite grain diameter before deformation, ϵ is the strain, and C, m, and n are constants. The equation can be used for optimizing the deformation schedule to achieve the finest austenite grain sizes possible during hot working.

OUTPUTS

and

INTERACTIONS

SELECTED RECENT PUBLICATIONS*

1. Adam, G.; Siewert, T. A., On-line arc welding data acquisition and analysis system, Recent Trends in Welding Science and Technology, ed. S.A. David and J.M. Vitek, ASM International, Metals Park, Ohio, p. 979–984, 1990.

2. Adam, G.; Siewert, T. A., Sensing of GMAW droplet transfer modes for a Mil 100S-1 electrode, Welding Journal, 69, March 1990, p. 103-s–108-s.

3. Berger, J. R.; Dally, J. W., A spatially overdetermined analysis for propagation toughness using strain gages, Mechanics Research Communications, Vol. 17, No. 2, p. 93–100, 1990.

4. Berger, J. R.; Dally, J. W.; Sanford, R. J., Determining the dynamic stress intensity factor with strain gages using a crack tip locating algorithm, Eng. Fract. Mech., Vol. 36, No. 1.

5. Berger, J.R. and Dally, J.W., Study of Static and Dynamic Fracture Using Strain Measurements, NISTIR 3952, 1990.

6. Berger, J.R.; Dally, J.W.; deWit, R.; Fields, R., A Strain Gage Analysis of Fracture in Wide Plate Tests of Reactor Grade Steel, submitted to ASME J. Pressure Vessel Tech.

7. Cheng, Y.W.; Sargent, C.L., Data Reduction and Analysis Procedures Used in NIST's Thermomechanical Processing Research, NISTIR 3950, August 1990.

8. Clark, A.V.; Thompson, R.B.; Li, Y.; Reno, R.C.; Blessing, G.V.; Mitrakovic, D.V.; Schramm, R.E.; Matlock, D., Ultrasonic Measurement of Sheet Steel Texture and Formability: Comparison with Neutron Diffraction and Mechanical Measurements, accepted for publication in Research in Nondestructive Evaluation.

9. Thompson, R.B.; Clark, A.V., Jr., Ultrasonic Characterization of Texture: Basic Science and Technology Transfer, Trans., Proceedings of ASM/TMS Symposium, October 1989.

10. Datta, S. K.; Ledbetter, H. M., Fiber-reinforced composites: models for macroscopic elastic constants, Dynamic Elastic Modulus Measurements in Materials, ASTM STP 1045 (ASTM, Philadelphia, 1990), p. 120–134.

11. Datta, S.; Ledbetter, H.; Taya, M., Elastic constants of SiC_W/Al_2O_3 composites: Measurements and modeling, in Nondestructive Characterization of Materials IV (Plenum, New York, 1990) forthcoming.

---

*Papers that were published or accepted for publication by the Editorial Review Boards of the National Institute of Standards and Technology during fiscal year 1990.

12. Dodds, R.H., Jr.; Read, D.T. Experimental and numerical studies of the J-integral for a surface flaw, International Journal of Fracture 43: 47–67, 1990.

13. Fisher, R. A.; Kim, S.; Wu, Y.; Phillips, N. E.; Ledbetter, H. M.; Togano, K., Specific heat of the high-T_c superconductor $(Bi_{1.66}Pb_{0.34})Ca_2Sr_3O_{10}$, Physica C 162–164, 502–403 (1989).

14. Fitting, D. W.; Clark, A. V., Monitoring of anisotropic material elastic properties using ultrasonic receiving arrays, Nondestructive Characterization of Materials, P. Höller, V. Hauk, G. Dobmann, C. Ruud and R. Green, eds., Springer-Verlag, Berlin, 1989.

15. Heyliger, P.; Ledbetter, H.; Austin, M., Resonating-orthotropic-cube method for elastic constants, Dynamic Elastic Modulus Measurements in Materials, ASTM STP 1045 (ASTM, Philadelphia, 1990), p. 100–109.

16. Kriz, R. D.; McColskey, J. D., Mechanical properties of alumina/PEEK unidirectional composite: compression, shear, and tension, Advances in Cryogenic Engineering, Vol. 36, Plenum Press, New York, 1990.

17. Kriz, R.D.; McColskey, J.D., Mechanical Properties of Alumina Fiber-Reinforced PEEK Thermal Plastic at Low Temperatures, NISTIR 3951, 1990.

18. Ledbetter, H.; Datta, S.; Kriz, R., Elastic constants of an Al_2O_3(fiber)/PEEK composite: Measurements, modeling, and low temperatures, in Nondestructive Characterization of Materials (Plenum, New York, 1991), forthcoming.

19. Ledbetter, H.; Datta, S., Elastic constants of a tungsten-particle copper-matrix composite, Japan Soc. Mech. Eng., forthcoming.

20. Ledbetter, H., Ultrasonic-wave studies of the new high-T_c metal-oxide superconductors, Elastic Waves and Ultrasonic Nondestructive Evaluation (Elsevier, Amsterdam, 1990), p. 345–350.

21. Ledbetter, H.; Lei, M.; Kim, S., Elastic constants, Debye temperatures, and electron-phonon parameters of superconducting cuprates and related oxides, Phase Trans. 22, 61–70 (1990).

22. Ledbetter, H.; Kim, S. A.; Violet, C. E.; Thompson, J. D., Low-temperature elastic constants of polycrystalline La_2CuO_4 and $La_{1.85}Sr_{0.15}CuO_4$, Physica C 162-164, 460–461 (1989).

23. Weller, M.; Ledbetter, H. M., Mechanical loss in a glass-epoxy composite, J. Mater. Res. 5, 913–915 (1990).

24. Ledbetter, H., Monocrystal-polycrystal elastic-constant models, Dynamic Elastic Modulus Measurements in Materials, ASTM STP 1045 (ASTM, Philadelphia, 1990), p. 135–148.

25. Ledbetter, H.; Lei, M., Is $Y_1Ba_2Cu_3O_7$ stiff or soft? J. Mater. Res. 5, 241–244 (1990).

26. Ledbetter, H.; Lei, M., Madelung potentials and valences in the $Y_1Ba_2Cu_3O_7$ superconductor, Physica C 166, 483–485 (1990).

27. Almasan, C.; Datta, T.; Edge, R. D.; Jones, E. R.; Cable, J. W.; Ledbetter, H. M., Low-temperature phase and magnetic interactions in fcc Fe–Cr–Ni alloys, Journal. Mag. Mater. 80, 329–338 (1989).

28. Liu, S.; Siewert, T. A.; Lan, H.-G., Metal transfer mode in gas metal arc welding, in Welding Science and Technology, eds. S.A. David and J.M. Vitek, ASM International, Metals Park, Ohio, p. 475–480, 1990.

29. Ma, L.; Han, J. K.; Tobler, R. L.; Walsh, R. P.; Reed, R. P., Cryogenic fatigue of high-strength aluminum alloys and its correlations with tensile properties, Advances in Cryogenic Engineering, Vol. 36, Plenum Press, New York, R.P. Reed and F.R. Fickett, eds., 1990, pp. 1143–1150.

30. McCowan, C. N.; Siewert, T. A.; Olson, D. L., Stainless steel weld metal: Prediction of the ferrite content, Weld. Res. Counc., New York, Bulletin 342, pp. 1–36, 1989.

31. McCowan, C. N.; Siewert, T. A., Fracture toughness of 316L stainless steel welds at 4 K, Advances in Cryogenics Engineering, Vol. 36, Plenum Press, New York, pp. 1331–1337.

32. McHenry, H.I., Institute for Materials Science and Engineering, Materials Reliability Division, Technical Activities 1989, NISTIR 89-4149, 1990.

33. Mo, J.H.; Robinson, A.L.; Fitting, D.W.; Temy Jr., F.L.; and Carson, P.L., Micromachining for Improvement of Integrated Ultrasonic Transducer Sensitivity, IEEE Trans. Elec. Devices, 37(1), pp. 134–140, 1990.

34. Nakajima, H.; Yoshida, K.; Shimamoto, S.; Tobler, R. L.; Reed, R. P.; Walsh, R. P.; Purtscher, P. T., Round robin tensile and fracture toughness test results for CSUS-JN1 (Fe–25Cr–15Ni–0.35N) austenitic stainless steel at 4 K, Adv. Cryo. Eng.-Mater., Vol. 36, Plenum Press, New York, R.P. Reed and F.R. Fickett, eds., 1990, pp. 1069–1076.

35. Purtscher, P. T.; Ma, L.-M.; Mataya, M. C.; Reed, R. P., Effect of processing on 4-K mechanical properties of a microalloyed austenitic stainless steel, Adv. Cryo. Eng.-Mater., Vol. 36A, Plenum Press, New York, pp. 1291–1298.

36. Purtscher, P. T.; Austin, M. W.; McCowan, C.; Reed, R. P.; Walsh, R. P.; Dunning, J., Application of 9% Cr austenitic steels at cryogenic temperatures, Adv. Cryo. Eng.-Mater., Vol. 36A, Plenum Press, New York, pp. 1265–1272.

37. Rao, R. R.; Ledbetter, H. M., Fourth-order elastic constants of β-brass, Int. J. Thermophys. 10, 899–902 (1989).

38. Read, D.T.; Pfuff, M., Potential drop in the center-cracked panel with asymmetric crack extension, Submitted to Int. J. Fract.

39. Reed, R. P.; Simon, N. J., Discontinuous yielding during tensile tests at low temperatures, Advances in Cryogenic Engineering-Materials, Vol. 36, Plenum Press, New York, 1077–1086 (1990).

40. Reed, R. P.; Simon, N. J.; Walsh, R. P., Creep of copper: 4 to 295 K, Advances in Cryogenic Engineering-Materials, Vol. 36, Plenum Press, New York, 1175–1184 (1990).

41. Reed, R. P.; Walsh, R. P.; Tobler, R. L., The effect of strain rate on tensile properties at 4 K of a VAMAS round-robin austenitic steel, Advances in Cryogenic Engineering-Materials, Vol. 36, Plenum Press, New York, 1061–1068 (1990).

42. Reed, R. P.; Lee, H. M.; Han, J. K., The load-control tensile behavior of austenitic steels at low temperatures, Advances in Cryogenic Engineering-Materials, Vol. 36, Plenum Press, New York, 1273–1282 (1990).

43. Reed, R.P.; Simon, N.J.; McColskey, J.D.; Berger, J.R.; McCowan, C.N.; Bransford, J.W.; Drexler, E.S.; Walsh, R.P., Aluminum Alloys for ALS Cryogenic Tranks: Oxygen Compatibility Interim Report, submitted to the USAF for publication.

44. Reed, R.P.; Simon, N.J.; McColskey, J.D.; McCowan, C.N.; Drexler, E.S., Aluminum Alloys for ALS Cryogenic Tanks: Oxygen Compatibility Final Report, submitted to the USAF for publication.

45. Reed, R.P.; R.L. Tobler, editors, Materials Studies for Magnetic Fusion Energy Applications at Low Temperatures – XII, NISTIR 89-3931, 1989.

46. Reed, R.P.; McCowan, C.N.; McColskey, J.D.; Simon, N.J.; Macro- and Microreactions in Mechanical-Impact Tests of Aluminum Alloys, Flammability and Sensitivity of Materials in Oxygen-Enriched Atmospheres: 5th Vol., ASTM STP 1111, J.M. Stoltzfus, ed., Phil., PA, forthcoming.

47. Reed, R.P.; Simon, N.J.; Berger, J.R.; McColskey, J.D.; Influence of Specimen Absorbed Energy in LOX Mechanical-Impact Tests, Flammability and Sensitivity of Materials in Oxygen-Enriched Atmospheres, 5th Vol., ASTM STP 1111, J.D. Stoltzfus, ed., Phila., PA, forthcoming.

48. Rosenthal, Y. A.; Tobler, T. L.; Purtscher, P. T., J_{Ic} data analysis with a negative crack growth correction procedure, J. Testing Evaluation, Journal of Testing and Evaluation, Vol. 18, No. 4, 1990, pp. 301–304.

49. Sanford, R. J.; Dally, J. W.; Berger, J. R., An improved strain gage method for measuring K_{ID} for a propagating crack, J. Strain Analysis, Vol. 25, No. 3, p. 177–183, 1990.

50. Schramm, R. E.; Shull, P.J.; Clark, A.V.; Mitrakovic, D.V. EMAT examination for cracks in railroad wheel treads. Conference proceedings, August 9–12, 1988, Urbana, Illinois, ed. H.L.M. dos Reis, Hemisphere Publishing, NY (1990), pp. 373–380.

51. Schramm, R.E.; Shull, P.J.; Clark, Jr., A.V.; Mitrakovic, D.V., Crack inspection of railroad wheel treads by EMATs. Nondestructive Characterization of Materials: Proceedings of the Third International Symposium, 3–6 October, 1988, Saarbrücken, Federal Republic of Germany, eds. P. Höller, V. Hauk, G. Dobmann, C.O. Ruud, R.E. Green, Springer-Verlag, Heidelberg (1989), pp. 421–428.

52. Siewert, T.A.; McCowan, C.N.; Vigliotti, D.P., Cryogenic material properties of stainless steel tube-to-flange welds, Cryogenics, 1990, p. 356–364.

53. Siewert, T. A., Standards for real-time radiography — National Bureau of Standards. Proceedings of Real-Time Imaging Topicals, Cincinnati, July 26–28, 1988, American Society for Nondestructive Testing, Columbus, Ohio, 1988.

54. Siewert, T.A., Review of 1986 workshop: Computerization of Welding Information. Computerization of Welding Data — Proceedings of the Conference and Workshop, October 19–21, 1988, ed. T.A. Siewert, J.E. Jones, and H.G. Ziegenfuss, NISTSP 781, p. 9–16, 1990.

55. Siewert, T. A.; Adam, G., The use of a statistical software package for monitoring material quality, Intelligent Instruments and Computers, Vol. 7, No. 1, p. 14, January/February 1989.

56. Siewert, T. A.; McCowan, C. N.; Olson, D. L., Ferrite number prediction for stainless steel welds, Chapter in book published by American Society for Metals, in press.

57. Lin, S.; Siewert, T.A.; Adam, G.; Lan, H.-G., Arc Welding Process Control from Current and Voltage Signals, Computer Technology in Welding, The Welding Institute, Abington Hall, Abington, Cambridge, UK, p. 26–35, 1990.

58. Siewert, T.A.; McCowan, C.N., Development of an SMA Electrode to Match Type 316 LN Base Metal Cryogenic Properties, submitted to Cryogenics

59. Siewert, T.A.; Jones, J.E.; Ziegenfuss, H.G., eds. Computerization of Welding Data - Proceedings of the Conference and Workshop, NIST Spec. Publ. 781, 1990.

60. Siewert, T.A.; Franke, G.L., Analysis and Characterization of Commercial Welding Fluxes, Welding Journal, Vol. 69, July 1990, p. 247-s–255-s.

61. Siewert, T.A.; Fitting, D.W.; Shepherd, D.A.; Austin, M.W.; McCowan, C.N., An Image Quality Indicator Design for Radioscopy and Tomography, Rev. Progress in Quantitative Nondestructive Evaluation, 9, eds. D.O. Thompson and D.F. Chimenti, Plenum Press, New York 1990.

62. Siewert, T.A.; Houle, M.J., Summary of the 1989 International Institute of Welding Assembly — Commission V — Testing, Measurement, and Control of Welds, Materials Evaluation, 48, March 1990, p. 408—412.

63. Siewert, T.A., Standard Formats for Welding Property Data, submitted to Proc., Computerization of Welding Conference III, Ypsilanti, MI, September 12—14, 1990 (in press).

64. Simon, N.J.; Reed, R.P., Temperature Increases in Aluminum Alloys During Mechanical-Impact Tests for Oxygen Compatability, Flammability and Sensitivity of Materials in Oxygen Enriched Atmospheres: Vol. 5, ASTM STP 1111, J.M. Stoltzfus, ed., Amer. Soc. for Testing and Mater., Phil., forthcoming.

65. Simon, N.J.; McColskey, J.D.; Reed, R.P.; Gracia-Salcedo, C.M., Reaction Sensitivities of Al—Li Alloys and Alloy 2219 in Mechanical-Impact Tests, Flammability and Sensitivity of Materials in Oxygen-Enriched Atmospheres: Vol. 5, ASTM STP 1111. Joel M. Stolzfus, ed., Amer. Soc. for Testing and Mater., Phil., forthcoming.

66. Simon, N.J.; Drexler, E.S.; Reed, R.P., Review of Cryogenic Mechanical and Thermal Properties of Al—Li Alloys and Alloy 2219, submitted to the USAF for publication.

67. Tewary, V.K.; Heyliger, P.R.; Clark, A.V., Theory of Capacitive Probe Method for Noncontact Characterization of Dielectric Properties of Materials, submitted to the Journal of Materials Research.

68. Tewary, V.K. and Fuller, Jr., E.R.; A Relation Between the Surface Energy and the Debye Temperature for Cubic Solids, J. Materials Research, Vol. 5, p. 1118—1122 (1990).

69. Tewary, V.K. and Fortunko, C.M., Application of Time Dependent Green's Function Method to Scattering of Elastic Waves in Anisotropic Solids, Review of Progress in Quantitative Nondestructive Evaluation, Vol. 10, forthcoming.

70. Tewary, V.K.; Kriz, R.D., Effect of a Free Surface on Stress Distribution in a Bimaterial Composite, NIST SP 802, 1990.

71. Tewary, V.K. and Kriz, R.D., Stress Distribution in a Bimaterial Composite Containing a Free Surface, Proceedings of Workshop on Elasticity of Anisotropic Solids, Army Research Office, Research Triangle Park, NC, forthcoming.

72. Tewary, V.K., Green's Function for Generalized Hilbert Problem for Cracks and Free Surfaces in Composite Materials, submitted to Journal of Materials Research.

73. Tewary, V.K., Elastic Green's Function for a Bimaterial Composite Solid Containing a Free Surface Normal to the Interface, submitted to Journal of Materials Research.

74. Tewary, V.K. and Kriz, R.D., Generalized Plane Strain Analysis of a Bimaterial Composite Containing a Free Surface Normal to the Interface, submitted to Journal of Materials Research.

75. Tobler, R.L.; Shimada, M., Warm Precracking Effects on the 4-K Fracture Toughness of Two Austenitic Stainless Steels, submitted for publication, ASTM Journal of Testing and Evaluation.

76. Tobler, R.L.; Reed, R.P.; Hwang, I.S.; Morra, M.M.; Ballinger, R.G.; Nakajima, H.; Shimamoto, S., Charpy Impact Tests near Absolute Zero, Journal of Testing and Evaluation (accepted for Jan. 1991).

77. Tobler, R.L. and Reed, R.P., eds., Materials Studies for Magnetic Fusion Energy Applications at Low Temperatures-XIII, NISTIR 3944, September 1990.

78. Yukawa, S., Guidelines for pressure vessel safety assessment, NIST Special Publication 780, National Institute of Standards and Technology, Boulder, Colorado, April 1990.

SELECTED TECHNICAL AND PROFESSIONAL COMMITTEE LEADERSHIP

American Society for Testing and Materials
- E07.01: Nondestructive Evaluation
  - Task Force on Evaluation of Real-Time Systems
    - T. A. Siewert, Member
- E24.06.05: Fracture Testing of Welds
  - H. I. McHenry, Chairman
- E28.07: Impact Testing
  - T. A. Siewert, Chairman
- E28.10.02: Temperature Effects
  - R.L. Tobler, Task Group Leader

American Welding Society
- Technical Papers Committee
  - T. A. Siewert
- *Welding Journal*
  - H. I. McHenry, Reviewer
  - T. A. Siewert, Reviewer
- Conference on Computerization of Welding Data
  - Organizing Committee
    - T. A. Siewert

Colorado School of Mines
- T. A. Siewert, Adjunct Professor

International Institute of Welding
- Task Group for Elastic–Plastic Fracture-Mechanics Standard
  - D. T. Read

International Union of Theoretical and Applied Mechanics
- Organizing Committee
  - H. M. Ledbetter

Metallurgical Society
- Metallurgical Transactions
  - H. M. Ledbetter

National Academy of Science
- Materials Advisory Group of the Marine Board
  - T. A. Siewert

NIST–Boulder Editorial Review Board
- J. R. Berger

University of Colorado
- Department of Mechanical Engineering Graduate Faculty
  - H. M. Ledbetter, Adjunct Professor

Welding Research Council

- Data Base Task Group
  - T. A. Siewert
- Materials and Welding Procedures Subcommittee
  - T. A. Siewert
- University Research Committee
  - T. A. Siewert

AWARDS

Raymond E. Schramm received the Bronze Medal for work on ultrasonic systems for railway safety.

Ralph L. Tobler received ASTM E-28 Committee's award of appreciate in recognition of active participation in development and improvement of cryogenic test standards.

INDUSTRIAL AND ACADEMIC INTERACTIONS

Industrial Interactions

Alcoa

The Cryogenic Materials Group is evaluating the metallurgical and mechanical properties of two vintages of Al–Li alloys.

Bechtel

The Cryogenic Materials Group is conducting large-scale tests on composite materials for use in the superconducting magnetic energy storage system.

Chaparral Steel

Yi-Wen Cheng and Dominique Shepherd are working with Chaparral Steel to determine the influence of processing on the mechanical properties of new microalloyed bar steels.

Chrysler Corporation

Yi-Wen Cheng is working with Chrysler Motors Corporation to develop the metallurgical data needed for the direct forging of microalloyed bar steels.

Conoco

D. T. Read is working with Conoco to develop fiber optic techniques to detect damage in uniaxial composite rods being evaluated for use as tendons in tension-leg platforms.

Eaton Corporation

Yi-Wen Cheng is working with Eaton to develop the metallurgical data needed for the direct forging of microalloyed bar steels.

Ford Motor Company

A. V. Clark is working with Ford to develop an ultrasonic measurement of formability. NIST is developing the instrument and Ford the tooling for use in an on-line demonstration at a Ford stamping plant.

General Atomics

The Cryogenic Materials Group is conducting large-scale tests on composite materials for use in the superconducting magnetic energy storage system.

General Electric

T. A. Siewert is working with the Aircraft Engines Department of General Electric and the Army Materials Technology Laboratory to develop a military standard for radioscopic inspection.

Hercules

The NDE Group is working with Hercules on ultrasonic techniques for nondestructive evaluation of composites.

Lockheed

C. M. Fortunko is working with Lockheed to develop a new standard test block to calibrate transducers used to inspect composite materials.

Lukens Steel

Yi-Wen Cheng and Harry McHenry are working with Lukens Steel to qualify thermomechanically processed steels for use in Naval shipbuilding.

Martin-Marietta

The Cryogenic Materials Group is generating and compiling mechanical property data on a new Al–Li alloy.

McDonnell–Douglas

J. D. McColskey is measuring the mechanical properties of graphite/PEEK composites, which may be used on the national aerospace plane (NASP).

Minnesota Valley Engineering

R.L. Tobler works with J. Guzzo to develop improved methods of conducting impact tests at 20 and 4 K to be used in quality control of Dewar construction materials.

Newport News Shipbuilding

T. A. Siewert is working with Newport News Shipbuilding to develop electrodes for welding high strength steels.

Precision Acoustic Devices (PAD), Inc.

C. M. Fortunko is collaborating with PAD in the development of an air-coupled ultrasonic instrument for the nondestructive evaluation of composite materials.

Perkin Elmer

H. Ledbetter is studying the sound velocities, thermal expansivity, and electrical resistivity of pure beryllium at low temperatures for Perkin Elmer in Danbury, Connecticut. Initial sound-velocity results suggest an unexpected low-temperature transition.

SCM Metal Products

H. Ledbetter is studying the elastic constants of alumina-dispersion-strengthened copper that is manufactured at SCM Metal Products in Cleveland, Ohio. Because the alumina particles are so small (a few hundred angstroms), modeling this material presents an intriguing problem.

Torrington Company

Yi-Wen Cheng is working with Torrington Company to develop high-temperature, high-strain rate flow properties of bearing steels.

Union Pacific Railroad

R. E. Schramm is developing an instrument to embed in railroad track to be used for the roll-by inspection of wheels.

Welding Research Council

T. A. Siewert and D. P. Vigliotti evaluate welded samples for the Materials and Welding Procedures Committee as part of the WRC effort to develop prequalified welding procedures. The committee is composed of welding fabricators, inspection agencies, insurance companies, sheet-metal workers, and other representatives of the welding industry.

Academic Interactions

Colorado School of Mines

T. A. Siewert is working with S. Liu in the study of droplet transfer in the welding arc.

A. V. Clark collaborates with D. Matlock on texture and formability research using ultrasonics.

Colorado State University

H. Ledbetter collaborates with P. Heyliger (Civil Engineering Department) in studying the natural resonance of regular solids.

Davidson College

H. Ledbetter collaborates with L. Cain of the Physics Department at Davidson College in Davidson, North Carolina in austenitic-steel elastic constants.

Harvard University

I.-H. Lin completed a one-year sabbatical to study the fracture and deformation of electronic materials under the direction of Professor J. R. Rice.

Indian Institute of Technology (Madras)

H. Ledbetter collaborates with R. Rao (Physics) on higher-order elastic constants.

Institute of Metal Research (Shenyang, P. R. China)

H. Ledbetter collaborates with Y. Li in studying austenitic-steel elastic constants.

Institute of Metallurgy, ETH (Zurich)

H. Ledbetter collaborates with P. Uggowitzer in studying austenitic-steel elastic constants.

Iowa State University: Center for Advanced NDE, Ames Laboratories

A. V. Clark collaborates with R. B. Thompson on texture and formability using ultrasonics.

Massachusetts Institute of Technology

I.-H. Lin works with A. Argon in studying the brittle-to-ductile transition in cleavage fracture.

R.L. Tobler works with Dr. I.S. Hwang in studies to develop and evaluate impact tests of structural alloys near absolute zero.

Max-Planck-Institut für Metallforschung (Stuttgart, F. R. Germany)

H. Ledbetter collaborates with M. Weller to study the internal friction and dielectric constants of various materials.

National Research Institute for Metals (Tsukuba, Japan)

H. Ledbetter collaborates with T. Ogata to study low temperature magnetic field elastic-constant apparatus.

H. Ledbetter collaborates with K. Togano to study oxide-superconductor elastic constants.

R.L. Tobler works with K. Nagai to plan and execute international round-robin tests programs in support of cryogenic test standards.

Ohio State University

Vinod Tewary of Ohio State is a guest scientist working with C.M. Fortunko on modelling interface problems related to the fracture of composite materials.

Osaka University

H. Ledbetter collaborates with Y. Tsunoda (Physics Department) to study Cu(Fe) elastic constants.

A. V. Clark works with H. Fukuoka and M. Hirao on the development of ultrasonic measurement techniques for determining residual stress and texture.

Stanford University

A. V. Clark and P. J. Shull collaborate with B. A. Auld on capacitive array research.

C. M. Fortunko is collaborating with Professor B. T. Kuri-Yakub on the development of air-coupled ultrasonic transducers.

Tohoku University

H. Ledbetter collaborates with Y. Shindo of the Mechanical Engineering Faculty on waves in composites.

H. Ledbetter collaborates with M. Taya on composite-material elastic constants.

Tsinghua University

H. Ledbetter continues studies with Y. He (Physics Department): on oxide-superconductor elastic constants.

University of Arkansas

H. Ledbetter collaborates with Z. Zheng (Physics Department) on oxide-superconductor elastic constants.

University of Belgrade

D. Mitraković was a guest researcher at NIST in the Nondestructive Evaluation group, working on instrumentation for inspecting railroad wheels.

University of California

H. Ledbetter collaborates with R. Fisher in studying oxide-superconductor specific heat.

University of Colorado

H. Ledbetter and C.M. Fortunko collaborate with Professor S. Datta (Mechanical Engineering Department) on waves in heterogeneous media.

H. Ledbetter collaborates with Professor A. Hermann on oxide-superconductor elastic constants.

University of Geneva

H. Ledbetter continues studies with B. Seeber on the elastic constants of Chevrel-phase superconductors.

University of Hawaii

H. Ledbetter collaborates with M. Manghnani (Geophysics) to study pressure dependence of elastic constants of oxide superconductors.

University of Maryland

H. Ledbetter collaborates with R. Reno (Physics Department) on studies of the effects of texture on elastic constants.

J. R. Berger collaborates with J. W. Dally and R. J. Sanford (Mechanical Engineering Department) on studies of dynamic fracture and crack arrest in structural steels.

University of Michigan

D. W. Fitting is collaborating with researchers at the University of Michigan on the development of silicon-based acoustical arrays.

University of South Carolina

H. Ledbetter collaborates with T. Datta (Physics Department) on magnetic properties: steels and superconductors.

University of Stuttgart

H. Ledbetter collaborates with B. Gairola (Institute for Theoretical and Applied Physics) on graphite-fiber elastic constants.

H. Ledbetter collaborates with E. Kröner on monocrystal—polycrystal elastic constants

University of Tsukuba

H. Ledbetter collaborates with T. Suzuki (Applied Physics) on elastic constants: phase transitions.

H. Ledbetter collaborates with K. Otsuka (Materials Science), on the elastic constants of the monocrystal shape-memory alloy Cu—Al—Ni.

H. Ledbetter collaborates with M. Saito (Engineering Mechanics), on elastic constants of technical solids.

Yale University

H. Ledbetter collaborates with B. Adams on elastic-constants/texture relationships.

MATERIALS RELIABILITY DIVISION

H. I. McHenry, Chief
C. M. Fortunko, Deputy

K. S. Sherlock
Administrative Officer

H. M. Quartemont
Division Secretary

V.E. Ciaranello, D.T. Lewis, Group Secretaries

Cryogenic Materials
H.I. McHenry*

E. S. Drexler
J. D. McColskey
P. T. Purtscher
R. L. Santoyo
N. J. Simon
R. L. Tobler
R. P. Walsh
A. Bussiba-GR

Nondestructive Evaluation
A. V. Clark

S. R. Schaps
R. E. Schramm
Y. Berlinsky-GR
Y. Cohen - GR
D. V. Mitrakovic-GR

Composites
C.M. Fortunko*

D. W. Fitting
L. J. Bond-Grant
E. E. Jensen-S
M. C. Renken-S
V. Tewary-Grant

Welding
T. A. Siewert

M. W. Austin
R. B. Madigan
C. N. McCowan
T. P. Quinn
D. A. Shepherd
D. P. Vigliotti
M. A. Mornis-S

Thermomechanical Processing
Y. W. Cheng

R. Kuziak-GR
A. Tomer-GR

Physical Properties
H. M. Ledbetter

S. A. Kim
T. Ashizawa-GR
D. Balzar-GR
M. Foldeaki-GR
M. Lei-contract
S.-H. Lin-GR

Fracture
D. T. Read

J. R. Berger
I.-H. Lin
S. Yukawa
A. Preis-S
M. Szanto-GR

GR – guest researcher
S – student
* – Acting

U.S.DEPARTMENT OF COMMERCE
National Institute of Standards and Technology

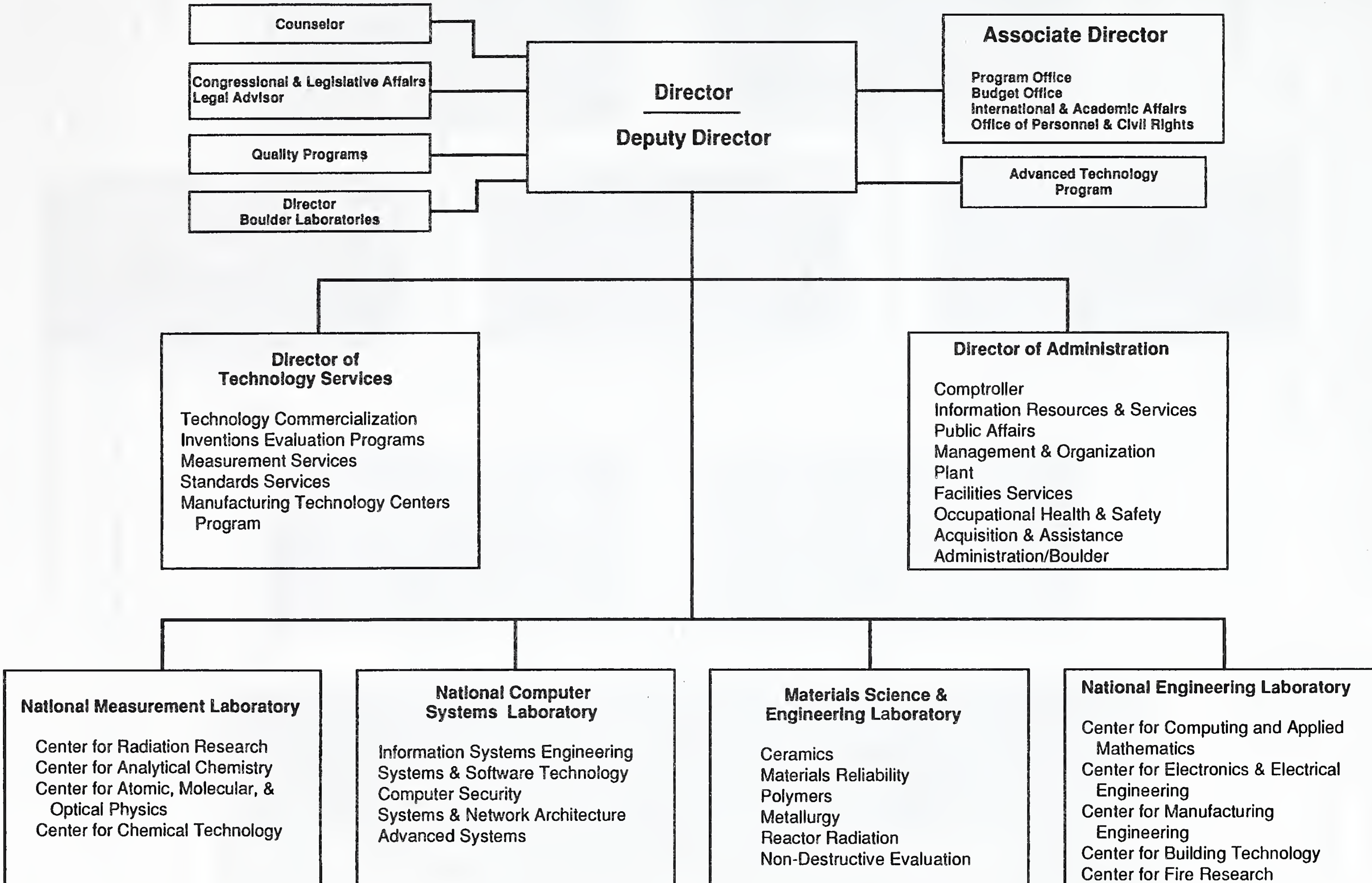

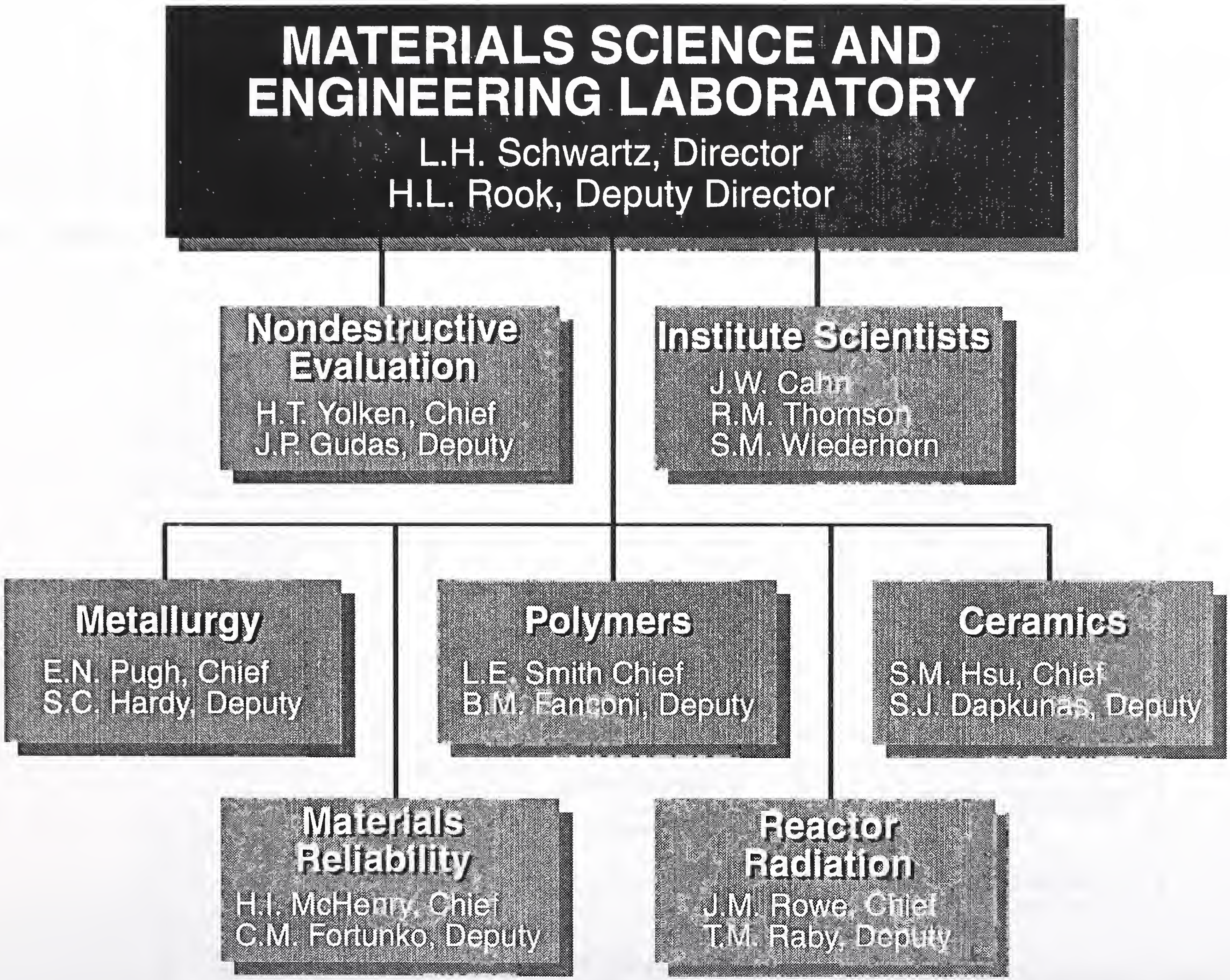
MATERIALS SCIENCE AND ENGINEERING LABORATORY
L.H. Schwartz, Director
H.L. Rook, Deputy Director
Nondestructive Evaluation
H.T. Yolken, Chief
J.P. Gudas, Deputy
Institute Scientists
J.W. Cahn
R.M. Thomson
S.M. Wiederhorn
Metallurgy
E.N. Pugh, Chief
S.C. Hardy, Deputy
Polymers
L.E. Smith Chief
B.M. Fanconi, Deputy
Ceramics
S.M. Hsu, Chief
S.J. Dapkunas, Deputy
Materials Reliability
H.I. McHenry, Chief
C.M. Fortunko, Deputy
Reactor Radiation
J.M. Rowe, Chief
T.M. Raby, Deputy

BL-114A
(5-90)

U.S. DEPARTMENT OF COMMERCE
NATIONAL INSTITUTE OF STANDARDS AND TECHNOLOGY

BIBLIOGRAPHIC DATA SHEET

1. PUBLICATION OR REPORT NUMBER
NISTIR 4395

2. PERFORMING ORGANIZATION REPORT NUMBER
B91-0043

3. PUBLICATION DATE
DECEMBER 1990

4. TITLE AND SUBTITLE
Materials Science and Engineering Laboratory
Materials Reliability Division
Technical Activities 1990

5. AUTHOR(S)
Harry I. McHenry, Editor

6. PERFORMING ORGANIZATION (IF JOINT OR OTHER THAN NIST, SEE INSTRUCTIONS)
U.S. DEPARTMENT OF COMMERCE
NATIONAL INSTITUTE OF STANDARDS AND TECHNOLOGY
BOULDER, COLORADO 80303-3328

EARLY ASSIGNMENT OF NISTIR NO. 4395.

7. CONTRACT/GRANT NUMBER

8. TYPE OF REPORT AND PERIOD COVERED

9. SPONSORING ORGANIZATION NAME AND COMPLETE ADDRESS (STREET, CITY, STATE, ZIP)
Materials Reliability Division, 430
National Institute of Standards & Technology
325 Broadway
Boulder, CO 80303

10. SUPPLEMENTARY NOTES

11. ABSTRACT (A 200-WORD OR LESS FACTUAL SUMMARY OF MOST SIGNIFICANT INFORMATION. IF DOCUMENT INCLUDES A SIGNIFICANT BIBLIOGRAPHY OR LITERATURE SURVEY, MENTION IT HERE.)

This report describes the 1990 fiscal-year programs of the Materials Reliability Division of the Materials Science and Engineering Laboratory. It summarizes the principal accomplishments in three general research areas: materials performance, properties, and processing. The Fracture Mechanics, Fracture Physics, Nondestructive Evaluation, and Composite Materials Groups work together to detect damage in metals and composite materials and to assess the significance of the damage with respect to service performance. The Cryogenic Materials and Physical Properties Groups investigate the behavior of materials at low temperature and measure and model the physical properties of advanced materials, including composites, ceramics and the new high-critical-temperature superconductors. The Welding and Thermomechanical Processing Groups investigate the nonequilibrium metallurgical changes that occur during processing and affect the quality, microstructure, properties and performance of metals.

The report lists the division's professional staff, their research areas, publications, leadership in professional societies, and collaboration in research programs with industries and universities.

12. KEY WORDS (6 TO 12 ENTRIES; ALPHABETICAL ORDER; CAPITALIZE ONLY PROPER NAMES; AND SEPARATE KEY WORDS BY SEMICOLONS)
composites; cryogenic materials; deformation; fracture; metallurgy; nondestructive evaluation; physical properties; steels; thermomechanical processing; welding

13. AVAILABILITY

- [X] UNLIMITED
- [ ] FOR OFFICIAL DISTRIBUTION. DO NOT RELEASE TO NATIONAL TECHNICAL INFORMATION SERVICE (NTIS).
- [ ] ORDER FROM SUPERINTENDENT OF DOCUMENTS, U.S. GOVERNMENT PRINTING OFFICE, WASHINGTON, DC 20402.
- [X] ORDER FROM NATIONAL TECHNICAL INFORMATION SERVICE (NTIS), SPRINGFIELD, VA 22161.

14. NUMBER OF PRINTED PAGES
82

15. PRICE
A05

ELECTRONIC FORM